PHYSICAL REVIEW A **94**, 062340 (2016)

Experimental device-independent tests of classical and quantum entropy

Feng Zhu,[1] Wei Zhang,[1,*] Sijing Chen,[2] Lixing You,[2] Zhen Wang,[2] and Yidong Huang[1]
[1]*Tsinghua National Laboratory for Information Science and Technology, Department of Electronic Engineering, Tsinghua University, Beijing 100084, China*
[2]*State Key Laboratory of Functional Materials for Informatics, Shanghai Institute of Microsystem and Information Technology (SIMIT), Chinese Academy of Sciences, Shanghai 200050, China*
(Received 10 May 2016; published 30 December 2016)

In quantum information processing, it is important to witness the entropy of the message in the device-independent way which was proposed recently [R. Chaves, J. B. Brask, and N. Brunner, Phys. Rev. Lett. **115**, 110501 (2015)]. In this paper, we theoretically obtain the minimal quantum entropy for three widely used linear dimension witnesses, which is considered "a difficult question." Then we experimentally test the classical and quantum entropy in a device-independent manner. The experimental results agree well with the theoretical analysis, demonstrating that entropy is needed in quantum systems that is lower than the entropy needed in classical systems with the given value of the dimension witness.

DOI: 10.1103/PhysRevA.94.062340

I. INTRODUCTION

Device-independent quantum information processing is attractive and developing rapidly. It is independent of the internal working of the devices used in the implementation, based on the observed data without any reference on the states and measurements [1]. The influence of the imperfection of practical devices will be eliminated.

Tests of resources in quantum information are also proposed in a device-independent manner, in which the source and the detector in the prepare-and-measure scenario are regarded as "black boxes." For example, entanglement is a basic resource in quantum communication and quantum computation [2]. Tests of the entanglement in a device-independent manner have been theoretically analyzed [3–5] and experimentally demonstrated [6]. Dimension is another important resource for the system used in quantum information processing [7]. It can also be tested in a device-independent way [8–10] and has been demonstrated experimentally [11–14].

Entropy is an important fundamental resource which reveals the amount of information in communication tasks [15,16]. Device-independent tests of entropy were proposed recently [17]. These are realized by constructing two entropy witnesses. The first one is based on causal inference networks [18], in which the facets of the entropic cone can be characterized [19–21] by associating a directed acyclic graph. This is a general method and valid for systems with arbitrary finite dimensions. However, it has an important drawback in that it cannot discriminate the classical case from the quantum case, since the lower bounds of the classical and quantum entropy calculated in this way are the same. The other way is based on convex optimization techniques, which can reveal the difference between the classical entropy and the quantum entropy [17]. Utilizing the value of the dimension witness, the minimal classical entropy can be explicitly derived. An upper bound of the minimal quantum entropy can also be obtained using four-dimensional systems. Whether it is exactly the minimal quantum entropy has not been investigated, since it is not clear whether higher-dimensional systems can be used to reduce the quantum entropy.

In this article, we theoretically investigate the minimal quantum entropy in systems with arbitrary dimension for any linear dimension witness, showing that it cannot be reduced by using higher-dimensional systems and that it is lower than the minimal classical entropy with the given value of the dimension witness. The classical entropy and the quantum entropy are tested experimentally, demonstrating their significant difference.

II. SCENARIO

The prepare-and-measure scenario we consider is illustrated in Fig. 1. The state preparator with n buttons is shown by the left box. When button $x \in \{1,\dots,n\}$ is pressed, it emits a message M in the classical case or a state ρ_x in the quantum case. The right box is the measurement device with l buttons. When button $y \in \{1,\dots,l\}$ is pressed, it performs a measurement M_y on the input state, delivering the outcome $b \in \{-1,+1\}$. $P(b|x,y)$ represents the probability for yielding the result b when the measurement M_y is taken on the state ρ_x. The expectation value of the measurement result is $E_{xy} = P(+1|x,y) - P(-1|x,y)$.

The buttons x and y are pressed upon the observers' request while the probability distributions of $P(x)$ and $P(y)$ are uniform and independent, i.e., $P(x) = 1/n$ and $P(y) = 1/l$. In the case of a d-dimensional classical system, it obeys deterministic strategies labeled by λ in the spirit of the ontological model [22]. Hence, $E_{xy} = \sum_m \sum_\lambda E(y,m,\lambda)P(m|x,\lambda)q_\lambda$, where q_λ is the probability of the strategy λ, $\sum_\lambda q_\lambda = 1$, $P(m|x,\lambda) \in \{0,1\}$, and $E(y,m,\lambda) \in \{-1,+1\}$. The probability distribution of the message is $p_m = \sum_x \sum_\lambda P(m|x,\lambda)q_\lambda/n$, where $m \in \{0,\dots,d-1\}$. The Shannon entropy of the average message M is $H(M) = -\sum_{m=0}^{d-1} p_m \log_2 p_m$. In the case of a d-dimensional quantum system, $E_{xy} = \mathrm{tr}(\rho_x M_y)$, where the state ρ_x and the measurement M_y act on $\mathbb{C}^d$. The von Neumann entropy of the average emitted state is $S(\rho) = -\mathrm{tr}(\rho \log_2 \rho)$, where $\rho = \sum_x \rho_x/n$.

*zwei@tsinghua.edu.cn

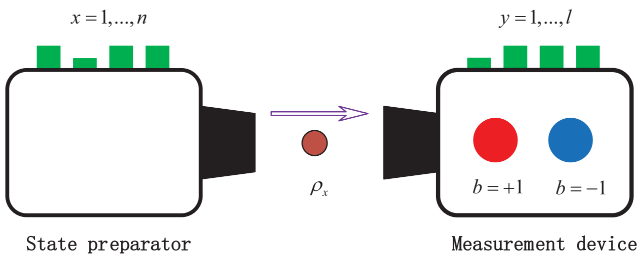

FIG. 1. Prepare-and-measure scenario.

III. THEORETICAL ANALYSIS

To investigate the gap between the minimal classical and quantum entropies, we propose and prove the following theorem to obtain the minimal quantum entropy with the given values of a linear dimension witness, w_d:

$$w_d = \sum_{x=1}^{n}\sum_{y=1}^{l}\alpha_{xy}\,\mathrm{tr}(\rho_x M_y). \tag{1}$$

Specifically, there are three widely used linear dimension witnesses, I_3, I_4, and R_4 [8,10]:

$$I_3 = E_{11} + E_{12} + E_{21} - E_{22} - E_{31}, \tag{2}$$

$$I_4 = E_{11} + E_{12} + E_{13} + E_{21} + E_{22} - E_{23} + E_{31} - E_{32} - E_{41}, \tag{3}$$

$$R_4 = E_{11} + E_{12} + E_{21} - E_{22} - E_{31} + E_{32} - E_{41} - E_{42}. \tag{4}$$

Theorem. Given the value of a linear dimension witness, $\sum_{x=1}^{n}\sum_{y=1}^{l}\alpha_{xy}\,\mathrm{tr}(\rho_x M_y) = w_d$, the minimum value of $S(\rho)$, where $\rho = (\rho_1 + \cdots + \rho_n)/n$, can be obtained when $\rho_k (1 \leqslant k \leqslant n)$ are all rank-1 and in $\mathbb{C}^n$.

Proof. See Appendix A. ■

According to the theorem, we only need to consider the rank-1 states ρ_x in an n-dimensional Hilbert space, which can be expressed as $\rho_x = |\psi_x\rangle\langle\psi_x|$, where

$$|\psi_1\rangle = (1,0,\ldots,0),$$
$$|\psi_2\rangle = (\cos\theta_{1,1}, e^{i\varphi_{1,1}}\sin\theta_{1,1}, 0, \ldots),$$
$$|\psi_3\rangle = (\cos\theta_{2,1}, e^{i\varphi_{2,1}}\sin\theta_{2,1}\cos\theta_{2,2}, e^{i\varphi_{2,2}}\sin\theta_{2,1}\sin\theta_{2,2}, \ldots),$$
$$\ldots$$
$$|\psi_n\rangle = \left(\cos\theta_{n-1,1}, \ldots, e^{i\varphi_{n-1,n-1}}\prod_{k=1}^{n-1}\sin\theta_{n-1,k}\right). \tag{5}$$

Since the eigenvalue of the measurement M_y is $+1$ or -1, the dimension witness has an upper bound of

$$w_d = \sum_{x=1}^{n}\sum_{y=1}^{l}\alpha_{xy}\,\mathrm{tr}(\rho_x M_y) \leqslant \sum_{y=1}^{l}\sum_{k}|\lambda_{yk}|, \tag{6}$$

where $\{\lambda_{yk}\}$ are the eigenvalues of $\rho^{(y)}$ and $\rho^{(y)} = \sum_{x=1}^{n}\alpha_{xy}\rho_x$. The minimal quantum entropies with the given value of $\sum_{y=1}^{l}\sum_k|\lambda_{yk}|$ are obtained for the cases of I_3, I_4, and R_4 numerically using fmincon in MATLAB. The calculation results show that the minimal quantum entropy is a monotone increasing function of $\sum_{y=1}^{l}\sum_k|\lambda_{yk}|$. Due to Eq. (6), this function also expresses the relation between the minimal quantum entropy and the given value of the dimension witness. It is indicated by the blue curves in Figs. 2(a)–2(c). On the other hand, the minimal classical entropy with given values of the dimension witnesses I_3, I_4, and R_4 are shown explicitly in Ref. [17]. They are calculated and indicated by the red curves in Figs. 2(a)–2(c), respectively.

The differences between the minimal quantum and classical entropies are indicated by the green curves in Figs. 2(d)–2(f), which show that the minimal quantum entropy is lower than the minimal classical entropy with the given value of the dimension witness. The maximum differences are presented in Table I. The details about the states ρ_x, the measurements M_y, the deterministic expectation values $E_{m,y}^{(\lambda)}$, the deterministic probability distribution $P_{m,x}^{(\lambda)}$, and the probability of strategy q_λ to realize the maximum differences for the dimension witnesses are shown in Appendix B.

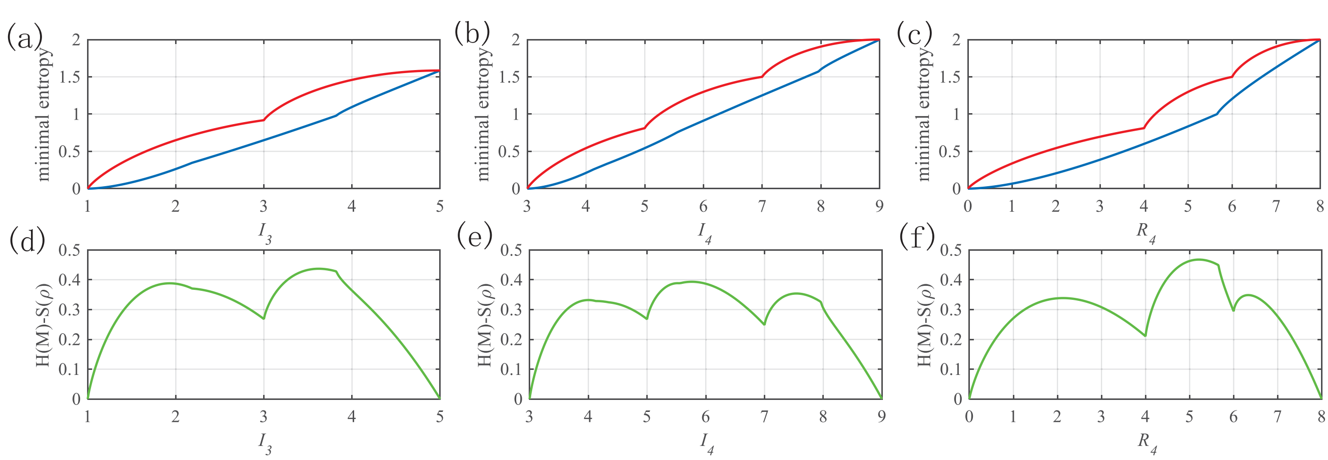

FIG. 2. The minimal classical (red) and quantum (blue) entropies with the given values of different dimension witnesses. Panels (a), (b), and (c) are the results for the dimension witnesses I_3, I_4, and R_4. Panels (d), (e), and (f) are the differences between the minimal classical and quantum entropies for each dimension witness. The unit of the longitudinal coordinates in all figures is bit.

TABLE I. Maximum differences between minimal quantum and classical entropies for I_3, I_4, and R_4.

	$H(M)$(bit)	$S(\rho)$(bit)	$H(M)-S(\rho)$(bit)
$I_3 = 3.622$	1.334	0.897	0.437
$I_4 = 5.760$	1.223	0.829	0.394
$R_4 = 5.211$	1.356	0.888	0.468

IV. EXPERIMENTAL TESTS

We encode the information on polarizations of photon pairs [23–26] generated by the spontaneous four-wave-mixing in a piece of optical fiber [27–29], by which the three-dimensional system for the test of I_3 and the four-dimensional system for the tests of I_4 and R_4 are realized. The setup is shown in Fig. 3.

The state preparator in Fig. 3 emits the photon pairs with information encoded on their polarizations. The four basis states (denoted by $\{|0\rangle,|1\rangle,|2\rangle,|3\rangle\}$) are $\{|V\rangle_s|V\rangle_i,|H\rangle_s|V\rangle_i,|H\rangle_s|H\rangle_i,|V\rangle_s|H\rangle_i\}$, where s and i stand for the signal photon and the idler photon, and H and V stand for the horizontal and vertical polarization directions. Each state is prepared by rotating the angles of the quarter-wave plate and two half-wave plates in the preparator, which are denoted by $q_s^{(p)}$, $h_s^{(p)}$, and $h_i^{(p)}$. The state of the photon pair can be expressed as

$$\begin{aligned}|\psi\rangle = {} & \frac{1}{\sqrt{2}}\big[\cos\big(2q_s^{(p)}-2h_s^{(p)}\big)-i\cos 2h_s^{(p)}\big]\cos 2h_i^{(p)}|0\rangle \\ & + \frac{1}{\sqrt{2}}\big[\sin\big(2q_s^{(p)}-2h_s^{(p)}\big)-i\sin 2h_s^{(p)}\big]\cos 2h_i^{(p)}|1\rangle \\ & + \frac{1}{\sqrt{2}}\big[\sin\big(2q_s^{(p)}-2h_s^{(p)}\big)-i\sin 2h_s^{(p)}\big]\sin 2h_i^{(p)}|2\rangle \\ & + \frac{1}{\sqrt{2}}\big[\cos\big(2q_s^{(p)}-2h_s^{(p)}\big)-i\cos 2h_s^{(p)}\big]\sin 2h_i^{(p)}|3\rangle. \end{aligned} \tag{7}$$

It is used as a four-dimensional system for cases of I_4 and R_4. For the case of I_3, only the first three terms are used.

For the classical case, each state is prepared to be one of the basis states $\{|0\rangle, |1\rangle, |2\rangle$, or $|3\rangle\}$, which is perfectly distinguishable. For different strategies, different q_λ are realized by

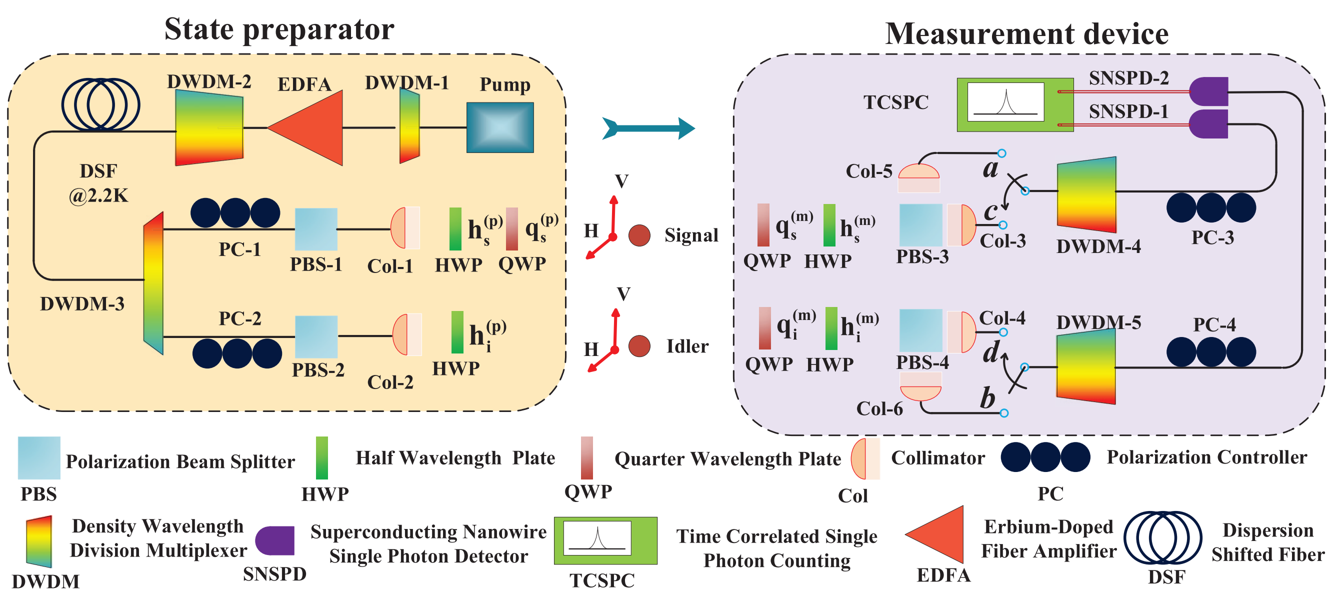

FIG. 3. The experimental setup. The left part is the state preparator. The linearly polarized pulsed pump light is generated by a passive mode-locked fiber laser with a repetitive rate of 40 MHz. Its linewidth is narrowed to 132 GHz by an optical filter (DWDM-1) with a central wavelength of 1552.52 nm. Then it is amplified by an erbium-doped fiber amplifier (EDFA). The noise produced by the EDFA is suppressed by another optical filter (DWDM-2). The correlated photon pairs are generated in a piece of dispersion-shifted fiber (DSF) with a length of 250 m. It is placed in a cryostat with the superconducting nanowire single-photon detectors (SNSPDs) used in this experiment and is cooled to 2.2 K to suppress the noise photons generated by the spontaneous Raman scattering. The signal and idler photons are selected and routed to two paths by the third optical filter (DWDM-3). Both of them have a linewidth of 63 GHz. Two polarization controllers (PC-1 and PC-2) and two polarization beam splitters (PBS-1 and PBS-2) are used to collimate the polarization of the signal and idler photons to the vertical direction. Then, the photons are coupled to free-space by two collimators (Col-1 and Col-2). The quarter-wave plate (QWP-$q_s^{(p)}$) and half-wave plates (HWP-$h_s^{(p)}$ and HWP-$h_i^{(p)}$) are used to encode the information on the state of the photon pairs. The right part is the measurement device. The input photons pass through two half-wave plates (HWP-$h_s^{(m)}$ and HWP-$h_i^{(m)}$) and two quarter-wave plates (QWP-$q_s^{(m)}$ and QWP-$q_i^{(m)}$), and then they are directed to four ports (a, b, c, and d) by two polarization beam splitters (PBS-3 and PBS-4). These components are used to realize the projection measurement of the biphoton states. Four collimators (Col-3 to Col-6) are used to couple the photons back to the fiber from different ports. The signal and idler photons from two specific ports are selected to be detected by two SNSPDs (fabricated by SIMIT, China). Their efficiencies and dark counts are about 40% and 80 Hz, respectively. Before the single-photon detection, two additional optical filters (DWDM-4 and DWDM-5) are used to filter out the noise and two polarization controllers (PC-3 and PC-4) are used to collimate the polarizations of the photons since the efficiencies of the SNSPDs are polarization dependent. The detection events of the SNSPDs are recorded by a time-correlated single-photon counting module (TCSPC, PicoQuant, PicoHarp 400).

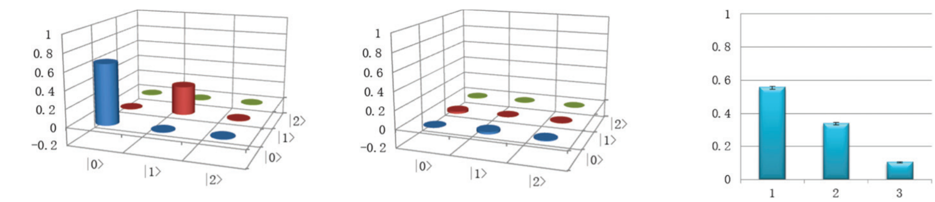

(a) (b) (c)

	Value$_{th}$	Value$_{exp}$
$w_d^{(c)}$	3.62	3.56(6)
$H(M)$ (bit)	1.33	1.34(2)
$w_d^{(q)}$	3.62	3.56(11)
$S(\rho)$ (bit)	0.90	0.94(3)

(d)

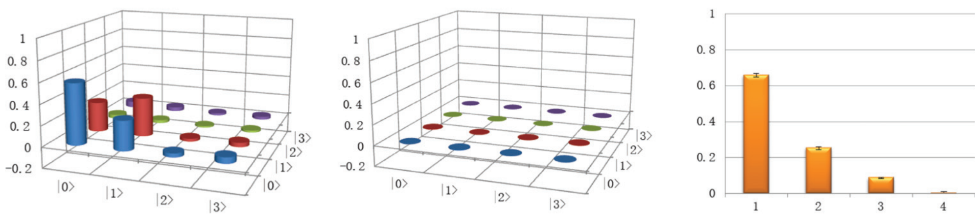

(e) (f) (g)

	Value$_{th}$	Value$_{exp}$
$w_d^{(c)}$	5.76	5.67(7)
$H(M)$ (bit)	1.22	1.22(6)
$w_d^{(q)}$	5.76	5.63(13)
$S(\rho)$ (bit)	0.83	0.88(7)

(h)

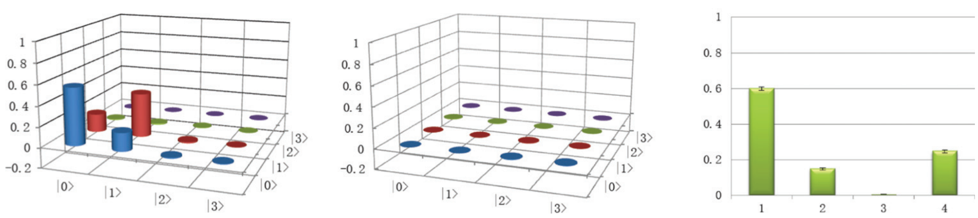

(i) (j) (k)

	Value$_{th}$	Value$_{exp}$
$w_d^{(c)}$	5.21	5.08(10)
$H(M)$ (bit)	1.36	1.38(4)
$w_d^{(q)}$	5.21	5.16(24)
$S(\rho)$ (bit)	0.89	0.96(7)

(l)

FIG. 4. The experimental results of the state ρ and the message M for I_3, I_4, and R_4. (a) Real part of ρ for I_3, (b) Imaginary part of ρ for I_3, (c) Distribution of M for I_3, (d) Results for I_3, (e) Real part of ρ for I_4, (f) Imaginary part of ρ for I_4, (g) Distribution of M for I_4, (h) Results for I_4, (i) Real part of ρ for R_4, (j) Imaginary part of ρ for R_4, (k) Distribution of M for R_4, and (l) Results for R_4.

different measurement time durations of corresponding states. The rotation angles of $q_s^{(p)}$, $h_s^{(p)}$, and $h_i^{(p)}$ for cases of I_3, I_4, and R_4 are shown in Appendix C.

The right part of Fig. 3 is the measurement device, which realizes the projection measurements of the state, by which the dimension witness and entropy for quantum and classical cases can be measured. The coincidence count of the two detectors is denoted by $D_{a,b}$ if the photons from port a and b are detected simultaneously. Similarly, $D_{a,d}$, $D_{c,b}$, and $D_{c,d}$ are the coincidence counts of the photons from the corresponding ports. For the quantum dimension witness, $P(-1|x,y)$ is obtained by $D_{a,b}$, and $P(+1|x,y)$ is obtained by $D_{a,d}$, $D_{c,b}$, and $D_{c,d}$. The projection state $|m_y\rangle$ is produced by rotating angles of two quarter-wave plates and two half-wave plates in the measurement device, which are denoted by $q_s^{(m)}$, $q_i^{(m)}$, $h_s^{(m)}$, and $h_i^{(m)}$, respectively. $|m_y\rangle$ can be expressed as

$$\begin{aligned}|m_y\rangle = {} & \tfrac{1}{2}\big[\cos\big(2q_s^{(m)} - 2h_s^{(m)}\big) + i\cos 2h_s^{(m)}\big]\big[\cos\big(2q_i^{(m)} - 2h_i^{(m)}\big) + i\cos 2h_i^{(m)}\big]|0\rangle + \tfrac{1}{2}\big[\sin\big(2q_s^{(m)} - 2h_s^{(m)}\big) + i\sin 2h_s^{(m)}\big] \\ & \times \big[\cos\big(2q_i^{(m)} - 2h_i^{(m)}\big) + i\cos 2h_i^{(m)}\big]|1\rangle + \tfrac{1}{2}\big[\sin\big(2q_s^{(m)} - 2h_s^{(m)}\big) + i\sin 2h_s^{(m)}\big]\big[\sin\big(2q_i^{(m)} - 2h_i^{(m)}\big) + i\sin 2h_i^{(m)}\big]|2\rangle \\ & + \tfrac{1}{2}\big[\cos\big(2q_s^{(m)} - 2h_s^{(m)}\big) + i\cos 2h_s^{(m)}\big]\big[\sin\big(2q_i^{(m)} - 2h_i^{(m)}\big) + i\sin 2h_i^{(m)}\big]|3\rangle. \end{aligned} \quad (8)$$

For the case of I_3, only the first three terms are used.

For the measurement of the quantum entropy witness, the states are reconstructed by quantum state tomography [24–26] which is realized by the detection events $D_{a,b}$ under different projection states. The details about the rotation angles of $h_s^{(m)}$, $q_s^{(m)}$, $h_i^{(m)}$, and $q_i^{(m)}$ for the quantum dimension witness and entropy are shown in Appendix C. For the classical dimension witness and entropy, the angles of $h_s^{(m)}$, $q_s^{(m)}$, $h_i^{(m)}$, and $q_i^{(m)}$ are all set to 0°. The measurement settings are reduced to an arrangement in which each coincidence count indicates a specific basis state, i.e., $|0\rangle \to D_{a,b}$, $|1\rangle \to D_{c,b}$, $|2\rangle \to D_{c,d}$, and $|3\rangle \to D_{a,d}$.

In the experiment, both the signal and idler photon count rates are about 19 kHz. The coincidence count rate is about $900\,\text{s}^{-1}$. The generation rate of the photon pairs is a little less than 0.01/pulse and the coincidence and accidence ratio (CAR) is higher than 100. Both the collection efficiencies of the signal and idler photons are about 5%, including the optical losses and the detector efficiencies. The time window of the coincidence counting is 300 ps. For the quantum case, each counting time of an event E_{xy} is 30 s. For the classical case, the total counting time of each event E_{xy} is 30 s, and the counting time for each strategy λ is $q_\lambda \times 30$ s.

The experimental results are shown in Fig. 4. Figures 4(a) and 4(b) are the real and imaginary parts of the density matrix ρ for the case of I_3, which is reconstructed by the measurement of quantum state tomography. Figure 4(c) is the measured distribution of message M for the case of I_3.

The quantum entropy $S(\rho)$ and the classical entropy $H(M)$ are calculated according to Figs. 4(a), 4(b), and 4(c) and shown in Fig. 4(d), with the experimental results of quantum and classical dimension witnesses ($w_d^{(q)}$ and $w_d^{(c)}$) for the case of I_3. The theoretical values of $S(\rho)$, $H(M)$, $w_d^{(q)}$, and $w_d^{(c)}$ are also listed in Fig. 4(d) for comparison. For the cases of I_4 and R_4, the corresponding results are shown in Figs. 4(e)–4(h) and Figs. 4(i)–4(l), respectively. The unideal factors in the experiment are analyzed. The errors of the experiment results are calculated and shown in Figs. 4(d), 4(h), and 4(l), considering the error sources of the limited angle precision of the polarization components, the imperfection of the polarization splitting, and the propagated Poissonian counting statistics of the detection events. It can be seen that the experimental results agree well with the theoretical expectations, showing that the minimal quantum entropy is lower than the minimal classical entropy with the given values of the dimension witnesses in all the cases.

V. DISCUSSION

In the theoretical analysis we have proved that the use of a system with a dimension higher than n is not helpful to reduce the minimal quantum entropy with the given values of the linear dimension witness $\sum_{x=1}^{n}\sum_{y=1}^{l}\alpha_{xy}\,\mathrm{tr}(\rho_x M_y)$. A related question is the following: if the given value of the dimension witness can be obtained by a d-dimensional system, where $d < n$, can the minimal value of $S(\rho)$ also be obtained by the d-dimensional system? On the other hand, we have calculated the minimal classical entropy according to Eq. (11) in Ref. [17] for the dimension witnesses I_3, I_4, and R_4 in the theoretical part of this paper. However, for an arbitrary linear dimension witness, could the minimal classical entropy be obtained in the same way? We find that the answer to two of the above questions is "no." We list counterexamples for them in Appendix D. It can be expected that α_{xy} would determine whether they hold or not; however, the conditions of α_{xy} to support them are not clear. This is an interesting open problem.

VI. CONCLUSION

We propose and prove a theorem which claims that the minimal value of $S(\rho)$ with the given values of the linear dimension witness $\sum_{x=1}^{n}\sum_{y=1}^{l}\alpha_{xy}\,\mathrm{tr}(\rho_x M_y)$ can be obtained in $\mathbb{C}^n$. This theorem is used to obtain the minimal quantum entropy for I_3, I_4, and R_4. With the minimal classical entropy indicated in Ref. [17], the differences between the minimal quantum and classical entropies are illustrated. Then we experimentally verify it by a telecom band biphoton system, in which the photon pair generation is based on the spontaneous four-wave mixing in optical fibers and the single-photon detections are based on SNSPDs. The qutrit and ququart are encoded on the polarizations of the photon pairs. The experimental results agree well with the theoretical values, demonstrating the reduction of communication entropy from the classical to the quantum system.

ACKNOWLEDGMENTS

This work was supported by the National Natural Science Foundation of China under Contracts No. 61575102, No. 91121022, and No. 61621064; the 973 Programs of China under Contracts No. 2013CB328700 and No. 2011CBA00303; the Tsinghua University Initiative Scientific Research Program under Contract No. 20131089382; the Strategic Priority Research Program (B) of the Chinese Academy of Sciences (Grant No. XDB04020100); and the Tsinghua National Laboratory for Information Science and Technology.

APPENDIX A: PROOF OF THE THEOREM

Lemma 1. Let M and ρ be an observable and a density matrix, respectively, where $\mathrm{rank}(\rho) = 2$. Then there exist two density matrices, ρ_0 and ρ_1, and two positive real numbers, μ_0 and μ_1, subject to

$$\mu_0 + \mu_1 = 1, \tag{A1}$$

$$\mu_0\rho_0 + \mu_1\rho_1 = \rho, \tag{A2}$$

$$\mathrm{rank}(\rho_0) = \mathrm{rank}(\rho_1) = 1, \tag{A3}$$

$$\mathrm{tr}(\rho_0 M) = \mathrm{tr}(\rho_1 M). \tag{A4}$$

Proof. Since the density matrix ρ is a Hermitian matrix, it can be represented by a diagonal matrix Λ under a specific complete orthogonal basis. Let the complete orthogonal basis and the diagonal matrix Λ be $\{|0\rangle,|1\rangle,|2\rangle,\ldots\}$ and $\mathrm{diag}\{\lambda_0,\lambda_1,\lambda_2,\ldots\}$, respectively. Since $\mathrm{rank}(\rho) = 2$, without loss of generality, let $\lambda_k = 0$ while $k \geqslant 2$. Then $\lambda_0 > 0$ and $\lambda_1 > 0$. Hence, the density matrix ρ can be written as $\rho = \lambda_0|0\rangle\langle 0| + \lambda_1|1\rangle\langle 1|$. The observable M can be written as $M = \sum_{k=0}\sum_{t=0} m_{kt}|k\rangle\langle t|$. Without loss of generality, let $m_{00} \geqslant m_{11}$.

Case 1. $m_{00} = m_{11}$. Let

$$\rho_0 = |0\rangle\langle 0|, \tag{A5}$$

$$\rho_1 = |1\rangle\langle 1|, \tag{A6}$$

$$\mu_0 = \lambda_0, \tag{A7}$$

$$\mu_1 = \lambda_1. \tag{A8}$$

Then Eq. (A1) holds since the trace of the density matrix ρ is 1. Equations (A2) and (A3) hold clearly. Equation (A4) holds since $\mathrm{tr}(\rho_0 M) = m_{00} = m_{11} = \mathrm{tr}(\rho_1 M)$.

Case 2. $m_{00} > m_{11}$. Let us define a function,

$$f(\theta) = m_{00}\cos^2\theta + m_{11}\sin^2\theta + (m_{10} + m_{01})\cos\theta\sin\theta - m_{00}\lambda_0 - m_{11}\lambda_1. \tag{A9}$$

Since $m_{00} > m_{11}$ and $\lambda_k > 0$ while $k\in\{0,1\}$, $f(0) = \lambda_1(m_{00} - m_{11}) > 0$ and $f(\frac{\pi}{2}) = f(-\frac{\pi}{2}) = -\lambda_0(m_{00} - m_{11}) < 0$. Since $f(\theta)$ is a continuous function, by the intermediate value theorem there exist $\theta_1 \in (0,\frac{\pi}{2})$ and $\theta_2 \in (-\frac{\pi}{2},0)$ such that $f(\theta_1) = f(\theta_2) = 0$.

Then let

$$\rho_0 = (\cos\theta_1|0\rangle + \sin\theta_1|1\rangle)(\cos\theta_1\langle 0| + \sin\theta_1\langle 1|), \tag{A10}$$

$$\rho_1 = (\cos\theta_2|0\rangle + \sin\theta_2|1\rangle)(\cos\theta_2\langle 0| + \sin\theta_2\langle 1|), \tag{A11}$$

$$\mu_0 = \frac{-\sin 2\theta_2}{\sin 2\theta_1 - \sin 2\theta_2}, \quad (A12)$$

$$\mu_1 = \frac{\sin 2\theta_1}{\sin 2\theta_1 - \sin 2\theta_2}. \quad (A13)$$

Since $2\theta_1 \in (0,\pi)$ and $2\theta_1 \in (-\pi,0)$, $\sin 2\theta_1 > 0$ and $\sin 2\theta_2 < 0$. It follows that $\mu_0 > 0$ and $\mu_1 > 0$. Furthermore, both Eqs. (A1) and (A3) hold clearly. Equation (A4) also holds since $\mathrm{tr}(\rho_0 M) = f(\theta_1) + \lambda_0 m_{00} + \lambda_1 m_{11} = \lambda_0 m_{00} + \lambda_1 m_{11} = f(\theta_2) + \lambda_0 m_{00} + \lambda_1 m_{11} = \mathrm{tr}(\rho_1 M)$.

Consider that

$$\begin{aligned} 0 &= \mu_0 0 + \mu_1 0 \\ &= \mu_0 f(\theta_1) + \mu_1 f(\theta_2) \\ &= (\mu_0 \cos^2\theta_1 + \mu_1 \cos^2\theta_2 - \lambda_0)m_{00} \\ &\quad + (\mu_0 \sin^2\theta_1 + \mu_1 \sin^2\theta_2 - \lambda_1)m_{11} \\ &= (\mu_0 \cos^2\theta_1 + \mu_1 \cos^2\theta_2 - \lambda_0)m_{00} \\ &\quad + [(1 - \mu_0 \cos^2\theta_1 - \mu_1 \cos^2\theta_2) - (1-\lambda_0)]m_{11} \\ &= (\mu_0 \cos^2\theta_1 + \mu_1 \cos^2\theta_2 - \lambda_0)(m_{00} - m_{11}) \\ &= \left(\frac{-\sin 2\theta_2 \cos^2\theta_1 + \sin 2\theta_1 \cos^2\theta_2}{\sin 2\theta_1 - \sin 2\theta_2} - \lambda_0\right)(m_{00} - m_{11}). \end{aligned} \quad (A14)$$

Then

$$\frac{-\sin 2\theta_2 \cos^2\theta_1 + \sin 2\theta_1 \cos^2\theta_2}{\sin 2\theta_1 - \sin 2\theta_2} = \lambda_0. \quad (A15)$$

$$\frac{-\sin 2\theta_2 \sin^2\theta_1 + \sin 2\theta_1 \sin^2\theta_2}{\sin 2\theta_1 - \sin 2\theta_2} = \lambda_1. \quad (A16)$$

Hence

$$\begin{aligned} \mu_0\rho_0 + \mu_1\rho_1 &= \mu_0(\cos\theta_1|0\rangle + \sin\theta_1|1\rangle)(\cos\theta_1\langle 0| \\ &\quad + \sin\theta_1\langle 1|) + \mu_1(\cos\theta_2|0\rangle + \sin\theta_2|1\rangle) \\ &\quad \times (\cos\theta_2\langle 0| + \sin\theta_2\langle 1|) \\ &= \frac{-\sin 2\theta_2 \cos^2\theta_1 + \sin 2\theta_1 \cos^2\theta_2}{\sin 2\theta_1 - \sin 2\theta_2}|0\rangle\langle 0| \\ &\quad + \frac{-\sin 2\theta_2 \sin^2\theta_1 + \sin 2\theta_1 \sin^2\theta_2}{\sin 2\theta_1 - \sin 2\theta_2}|1\rangle\langle 1| \end{aligned} \quad (A17)$$

Since Eqs. (A15)–(A17), Eq. (A2) holds. ■

Lemma 2. Let M and ρ be an observable and a density matrix, respectively, where $\mathrm{rank}(\rho) = n > 2$. Then there exist three density matrices, ρ_0, ρ_1, and ρ', and three positive real numbers, μ_0, μ_1, and μ', subject to

$$\mu_0 + \mu_1 + \mu' = 1, \quad (A18)$$

$$\mu_0\rho_0 + \mu_1\rho_1 + \mu'\rho' = \rho, \quad (A19)$$

$$\mathrm{rank}(\rho_0) = \mathrm{rank}(\rho_1) = 1, \quad (A20)$$

$$\mathrm{tr}(\rho_0 M) = \mathrm{tr}(\rho_1 M) = \mathrm{tr}(\rho M), \quad (A21)$$

$$\mathrm{rank}(\rho') < \mathrm{rank}(\rho). \quad (A22)$$

Proof. Since the density matrix ρ is a Hermitian matrix, it can be represented by a diagonal matrix Λ under a specific complete orthogonal basis. Let the complete orthogonal basis be $\{|0\rangle,|1\rangle,|2\rangle,\ldots,|n-2\rangle,|n-1\rangle,|n\rangle,\ldots\}$ and the diagonal matrix Λ be $\mathrm{diag}\{\lambda_0,\lambda_1,\lambda_2,\ldots,\lambda_{n-2},\lambda_{n-1},\lambda_n,\ldots\}$. Since $\mathrm{rank}(\rho) = n$, without loss of generality, let $\lambda_k = 0$ while $k \geqslant n$. Then $\lambda_k > 0$ while $0 \leqslant k \leqslant n-1$. Hence, the density matrix ρ can be written as $\rho = \sum_{k=0}^{n-1}\lambda_k|k\rangle\langle k|$. The observable M can be written as $M = \sum_{k=0}\sum_{t=0} m_{kt}|k\rangle\langle t|$. Let m_{ii} and m_{jj} be the maximum and minimum among the first n diagonal elements of the matrix of M; hence

$$m_{ii} = \max\{m_{00},\ldots,m_{n-1n-1}\}, \quad (A23)$$

$$m_{jj} = \min\{m_{00},\ldots,m_{n-1n-1}\}. \quad (A24)$$

It follows that

$$m_{ii} \geqslant m_{jj}. \quad (A25)$$

Case 1. $m_{ii} = m_{jj}$. Thus $m_{00} = m_{11} = \cdots = m_{n-1n-1}$. Let

$$\rho_0 = |i\rangle\langle i|, \quad (A26)$$

$$\rho_1 = |j\rangle\langle j|, \quad (A27)$$

$$\rho' = \frac{1}{1-\lambda_i-\lambda_j}\sum_{\substack{k=0\\ k\neq i\\ k\neq j}}^{n-1}\lambda_k|k\rangle\langle k|, \quad (A28)$$

$$\mu_0 = \lambda_i, \quad (A29)$$

$$\mu_1 = \lambda_j, \quad (A30)$$

$$\mu' = 1 - \lambda_i - \lambda_j. \quad (A31)$$

Since $\mathrm{rank}(\rho) > 2$, μ_0, μ_1, and μ' are all positive real numbers. ρ_0, ρ_1, and ρ' are density matrices since $\lambda_k \geqslant 0$ and $\sum_{k=0,k\neq i,k\neq j}^{n-1}\lambda_k = 1 - \lambda_i - \lambda_j$. Equations (A18)–(A20) hold clearly. $\mathrm{rank}(\rho') = n-2 < n = \mathrm{rank}(\rho)$; hence Eq. (A22) holds. $\mathrm{tr}(\rho_1 M) = m_{ii}$, $\mathrm{tr}(\rho_2 M) = m_{jj} = m_{ii}$, and $\mathrm{tr}(\rho M) = \sum_{k=0}^{n-1}\lambda_k m_{kk} = m_{ii}$ because $\sum_{k=0}^{n-1}\lambda_k = 1$ and $m_{00} = m_{11} = \ldots = m_{n-2n-2} = m_{n-1n-1}$. It follows that Eq. (A21) holds.

Case 2. $m_{ii} > m_{jj}$. Let us define a function,

$$F(\theta) = m_{ii}\cos^2\theta + m_{jj}\sin^2\theta + (m_{ji}+m_{ij})\cos\theta\sin\theta - \sum_{k=0}^{n-1} m_{kk}\lambda_k. \quad (A32)$$

Since $m_{ii} > m_{jj}$, $\lambda_k > 0$ while $0 \leqslant k \leqslant n-1$, and $\sum_{k=0}^{n-1}\lambda_k = 1$, $F(0) = m_{ii} - \sum_{k=0}^{n-1}\lambda_k m_{kk} > 0$, and $F(\frac{\pi}{2}) = F(-\frac{\pi}{2}) = m_{jj} - \sum_{k=0}^{n-1}\lambda_k m_{kk} < 0$. Since $F(\theta)$ is a continuous function, by the intermediate value theorem there exist $\theta_1 \in (0,\frac{\pi}{2})$ and $\theta_2 \in (-\frac{\pi}{2},0)$ such that $F(\theta_1) = F(\theta_2) = 0$.

Case 2.1. $(\sin 2\theta_1\cos^2\theta_2 - \sin 2\theta_2\cos^2\theta_1)/\lambda_i > (\sin 2\theta_1\sin^2\theta_2 - \sin 2\theta_2\sin^2\theta_1)/\lambda_j$. Let

$$\rho_0 = (\cos\theta_1|i\rangle + \sin\theta_1|j\rangle)(\cos\theta_1\langle i| + \sin\theta_1\langle j|), \quad (A33)$$

$$\rho_1 = (\cos\theta_2|i\rangle + \sin\theta_2|j\rangle)(\cos\theta_2\langle i| + \sin\theta_2\langle j|), \quad (A34)$$

$$\mu_0 = \lambda_i \frac{-\sin 2\theta_2}{\sin 2\theta_1 \cos^2\theta_2 - \sin 2\theta_2 \cos^2\theta_1}, \tag{A35}$$

$$\mu_1 = \lambda_i \frac{\sin 2\theta_1}{\sin 2\theta_1 \cos^2\theta_2 - \sin 2\theta_2 \cos^2\theta_1}, \tag{A36}$$

$$\mu' = 1 - \lambda_i \frac{\sin 2\theta_1 - \sin 2\theta_2}{\sin 2\theta_1 \cos^2\theta_2 - \sin 2\theta_2 \cos^2\theta_1}, \tag{A37}$$

$$\rho' = \frac{1}{\mu'}\left[\left(\sum_{\substack{k=0\\k\neq i\\k\neq j}}^{n-1} \lambda_k |k\rangle\langle k|\right) + \left(\lambda_j - \lambda_i \frac{\sin 2\theta_1 \sin^2\theta_2 - \sin 2\theta_2 \sin^2\theta_1}{\sin 2\theta_1 \cos^2\theta_2 - \sin 2\theta_2 \cos^2\theta_1}\right)|j\rangle\langle j|\right]. \tag{A38}$$

Since $2\theta_1 \in (0,\pi)$ and $2\theta_1 \in (-\pi,0)$, $\sin 2\theta_1 > 0$ and $\sin 2\theta_2 < 0$. It follows that $\mu_0 > 0$ and $\mu_1 > 0$. Furthermore, $\mu' > 0$ since

$$\begin{aligned}\mu' &= 1 - \lambda_i \frac{\sin 2\theta_1 - \sin 2\theta_2}{\sin 2\theta_1 \cos^2\theta_2 - \sin 2\theta_2 \cos^2\theta_1}\\
&= \left(\sum_{\substack{k=0\\k\neq i\\k\neq j}}^{n-1} \lambda_k + \lambda_j + \lambda_i\right) - \lambda_i \frac{\sin 2\theta_1 - \sin 2\theta_2}{\sin 2\theta_1 \cos^2\theta_2 - \sin 2\theta_2 \cos^2\theta_1}\\
&= \left(\sum_{\substack{k=0\\k\neq i\\k\neq j}}^{n-1} \lambda_k\right) + \left(\lambda_j - \lambda_i \frac{\sin 2\theta_1 \sin^2\theta_2 - \sin 2\theta_2 \sin^2\theta_1}{\sin 2\theta_1 \cos^2\theta_2 - \sin 2\theta_2 \cos^2\theta_1}\right)\\
&> \lambda_j - \lambda_i \frac{\sin 2\theta_1 \sin^2\theta_2 - \sin 2\theta_2 \sin^2\theta_1}{\sin 2\theta_1 \cos^2\theta_2 - \sin 2\theta_2 \cos^2\theta_1} > 0.\end{aligned} \tag{A39}$$

Since ρ' is a semipositive definite Hermitian matrix and $\mathrm{tr}(\rho') = \mu'/\mu' = 1$, ρ' is a density matrix. Equations (A18) and (A19) hold clearly. ρ_0 and ρ_1 are rank-1 density matrices; therefore Eq. (A20) holds. Equation (A21) also holds since $\mathrm{tr}(\rho_0 M) = F(\theta_1) + \sum_{k=0}^{n-1} \lambda_k m_{kk} = 0 + \mathrm{tr}(\rho M) = F(\theta_2) + \sum_{k=0}^{n-1} \lambda_k m_{kk} = \mathrm{tr}(\rho_1 M)$. $\mathrm{rank}(\rho') < n$ since ρ' doesn't have the term of $|i\rangle\langle i|$. Therefore Eq. (A22) holds.

Case 2.2. $(\sin 2\theta_1 \cos^2\theta_2 - \sin 2\theta_2 \cos^2\theta_1)/\lambda_i \leqslant (\sin 2\theta_1 \sin^2\theta_2 - \sin 2\theta_2 \sin^2\theta_1)/\lambda_j$. Let

$$\rho_0 = (\cos\theta_1 |i\rangle + \sin\theta_1 |j\rangle)(\cos\theta_1 \langle i| + \sin\theta_1 \langle j|), \tag{A40}$$

$$\rho_1 = (\cos\theta_2 |i\rangle + \sin\theta_2 |j\rangle)(\cos\theta_2 \langle i| + \sin\theta_2 \langle j|), \tag{A41}$$

$$\mu_0 = \lambda_j \frac{-\sin 2\theta_2}{\sin 2\theta_1 \sin^2\theta_2 - \sin 2\theta_2 \sin^2\theta_1}, \tag{A42}$$

$$\mu_1 = \lambda_j \frac{\sin 2\theta_1}{\sin 2\theta_1 \sin^2\theta_2 - \sin 2\theta_2 \sin^2\theta_1}, \tag{A43}$$

$$\mu' = 1 - \lambda_j \frac{\sin 2\theta_1 - \sin 2\theta_2}{\sin 2\theta_1 \sin^2\theta_2 - \sin 2\theta_2 \sin^2\theta_1}, \tag{A44}$$

$$\rho' = \frac{1}{\mu'}\left[\left(\sum_{\substack{k=0\\k\neq i\\k\neq j}}^{n-1} \lambda_k |k\rangle\langle k|\right) + \left(\lambda_i - \lambda_j \frac{\sin 2\theta_1 \cos^2\theta_2 - \sin 2\theta_2 \cos^2\theta_1}{\sin 2\theta_1 \sin^2\theta_2 - \sin 2\theta_2 \sin^2\theta_1}\right)|i\rangle\langle i|\right]. \tag{A45}$$

Equations (A18)–(A22) hold by a proof similar to Case 2.1. ■

Lemma 3. Let M and ρ be an observable and a density matrix, respectively. Then there exist density matrices $\{\rho_0, \ldots, \rho_{s-1}\}$ and positive real numbers $\{\nu_0, \ldots, \nu_{s-1}\}$ subject to

$$\sum_{k=0}^{s-1} \nu_k = 1, \tag{A46}$$

$$\sum_{k=0}^{s-1} \nu_k \rho_k = \rho, \tag{A47}$$

$$\mathrm{rank}(\rho_k) = 1 \quad \text{while } 0 \leqslant k \leqslant s-1, \tag{A48}$$

$$\mathrm{tr}(\rho_k M) = \mathrm{tr}(\rho M) \quad \text{while } 0 \leqslant k \leqslant s-1. \tag{A49}$$

Proof. Case 1. $\mathrm{rank}(\rho) = 1$. Let $\rho_1 = \rho$ and $\nu_1 = 1$. Equations (A46)–(A49) hold.

Case 2. $\mathrm{rank}(\rho) = 2$. Using Lemma 1, there exist ρ_0, ρ_1, μ_0, and μ_1, satisfying Eqs. (A1)–(A4). Let $\nu_0 = \mu_0$ and $\nu_1 = \mu_1$, then Eqs. (A46)–(A48) hold. Consider that

$$\begin{aligned}\mathrm{tr}(\rho M) &= \mathrm{tr}\{(\mu_0\rho_0 + \mu_1\rho_1)M\}\\
&= \mu_0\,\mathrm{tr}(\rho_0 M) + \mu_1\,\mathrm{tr}(\rho_1 M)\\
&= \mu_0\,\mathrm{tr}(\rho_0 M) + (1-\mu_0)\,\mathrm{tr}(\rho_1 M)\\
&= \mathrm{tr}(\rho_0 M),\end{aligned} \tag{A50}$$

then Eq. (A49) holds.

Case 3. $\mathrm{rank}(\rho) > 2$. Using Lemma 2, there exist ρ_0, ρ_1, ρ', μ_0, μ_1, and μ', satisfying Eqs. (A18)–(A22). If $\mathrm{rank}(\rho')$ is still larger than 2, using Lemma 2 again, there exist ρ_2, ρ_3, ρ'', μ_2, μ_3, and μ'', subject to

$$\mu_2 + \mu_3 + \mu'' = 1, \tag{A51}$$

$$\rho' = \mu_2\rho_2 + \mu_3\rho_3 + \mu''\rho'', \tag{A52}$$

$$\mathrm{rank}(\rho_2)=\mathrm{rank}(\rho_3)=1, \tag{A53}$$

$$\mathrm{tr}(\rho_2 M)=\mathrm{tr}(\rho_3 M)=\mathrm{tr}(\rho' M), \tag{A54}$$

$$\mathrm{rank}(\rho'')<\mathrm{rank}(\rho'). \tag{A55}$$

Repeat using Lemma 2 until $\mathrm{rank}(\rho'^{\cdots\prime})\leqslant 2$. This process takes finite time since the rank of a density matrix is a positive integer and $\mathrm{rank}(\rho)>\mathrm{rank}(\rho')>\mathrm{rank}(\rho'')>\dots$. At last, since $\mathrm{rank}(\rho'^{\cdots\prime})\leqslant 2$, $\rho'^{\cdots\prime}$ can be decomposed as the equations in Case 1 or Case 2. Then let $\nu_0=\mu_0$, $\nu_1=\mu_1$, $\nu_2=\mu_2\mu'$, $\nu_3=\mu_3\mu'$, $\nu_4=\mu_4\mu'\mu''$, $\nu_5=\mu_5\mu'\mu''$, and so on.

Considering Eqs. (A18) and (A51), Eq. (A46) holds since

$$\begin{aligned}1&=\mu_0+\mu_1+\mu'\\&=\mu_0+\mu_1+\mu'(\mu_2+\mu_3+\mu'')\\&=\mu_0+\mu_1+\mu'\mu_2+\mu'\mu_3+\mu'\mu''(\mu_4+\mu_5+\mu''')\\&=\nu_0+\nu_1+\nu_2+\nu_3+\nu_4+\nu_5+\cdots.\end{aligned} \tag{A56}$$

Because of Eqs. (A19) and (A52), Eq. (A47) can be derived using a method similar to Eq. (A56). Equation (A48) holds clearly.

We notice that

$$\begin{aligned}\mathrm{tr}(\rho' M)&=\mathrm{tr}\left(\frac{\rho-\mu_1\rho_1+\mu_2\rho_2}{\mu'}M\right)\\&=\frac{1}{\mu'}[\mathrm{tr}(\rho M)-\mu_1\,\mathrm{tr}(\rho_1 M)-\mu_2\,\mathrm{tr}(\rho_2 M)]\\&=\frac{1}{\mu'}[1-\mu_1-\mu_2]\,\mathrm{tr}(\rho M)\\&=\mathrm{tr}(\rho M).\end{aligned} \tag{A57}$$

Similar to Eq. (A57), it is easy to obtain that $\mathrm{tr}(\rho M)=\mathrm{tr}(\rho' M)=\mathrm{tr}(\rho'' M)=\cdots$. Then $\mathrm{tr}(\rho M)=\mathrm{tr}(\rho_1 M)=\mathrm{tr}(\rho_2 M)=\mathrm{tr}(\rho_3 M)=\mathrm{tr}(\rho_4 M)=\dots$, because of Eqs. (A21) and (A54). It follows that Eq. (A49) holds. ■

Theorem. Given the value of a linear dimension witness, $\sum_{x=1}^{n}\sum_{y=1}^{l}\alpha_{xy}\,\mathrm{tr}(\rho_x M_y)=w_d$, the minimum value of the Von Neumann entropy $S(\rho)$, where $\rho=(\rho_1+\cdots+\rho_n)/n$ can be obtained when $\rho_k(1\leqslant k\leqslant n)$ are all rank-1 and in $\mathbb{C}^n$.

Proof. Let $M^{(x)}=\sum_{y=1}^{l}\alpha_{xy}M_y$, then the dimension witness can be written as

$$\sum_{x=1}^{n}\mathrm{tr}(\rho_x M^{(x)})=w_d. \tag{A58}$$

Using Lemma 3, for ρ_x and $M^{(x)}$, there exist density matrices $\{\rho_{x,0},\dots,\rho_{x,s_x-1}\}$ and positive real numbers $\{\nu_{x,0},\dots,\nu_{x,s_x-1}\}$, subject to

$$\sum_{k_x=0}^{s_x-1}\nu_{x,k_x}=1, \tag{A59}$$

$$\sum_{k_x=0}^{s_x-1}\nu_{x,k_x}\rho_{x,k_x}=\rho, \tag{A60}$$

$$\mathrm{rank}(\rho_{x,k_x})=1\quad\text{while } 0\leqslant k_x\leqslant s_x-1, \tag{A61}$$

$$\mathrm{tr}(\rho_{x,k_x}M^{(x)})=\mathrm{tr}(\rho_x M^{(x)})\quad\text{while } 0\leqslant k_x\leqslant s_x-1. \tag{A62}$$

Then

$$\begin{aligned}&\sum_{k_1=0}^{s_1-1}\sum_{k_2=0}^{s_2-1}\cdots\sum_{k_n=0}^{s_n-1}\nu_{1,k_1}\nu_{2,k_2}\dots\nu_{n,k_n}\\&=\left(\sum_{k_1=0}^{s_1-1}\nu_{1,k_1}\right)\left(\sum_{k_2=0}^{s_2-1}\nu_{2,k_2}\right)\cdots\left(\sum_{k_n=0}^{s_n-1}\nu_{n,k_n}\right)\\&=1.\end{aligned} \tag{A63}$$

Furthermore

$$\begin{aligned}\rho&=\frac{1}{n}(\rho_1+\cdots+\rho_n)\\&=\frac{1}{n}\left[\left(\sum_{k_1=0}^{s_1-1}\nu_{1,k_1}\rho_{1,k_1}\right)+\left(\sum_{k_2=0}^{s_2-1}\nu_{2,k_2}\rho_{2,k_2}\right)+\cdots\right.\\&\quad\left.+\left(\sum_{k_n=0}^{s_n-1}\nu_{n,k_n}\rho_{n,k_n}\right)\right]\\&=\sum_{k_1=1}^{s_1}\sum_{k_2=1}^{s_2}\dots\sum_{k_n=1}^{s_n}\nu_{1,k_1}\nu_{2,k_2}\dots\nu_{n,k_n}\\&\quad\times\left[\frac{1}{n}(\rho_{1,k_1}+\cdots+\rho_{n,k_n})\right].\end{aligned} \tag{A64}$$

Since $(\rho_{1,k_1}+\cdots+\rho_{n,k_n})/n$ is also a density matrix and from Eq. (2.2) on page 237 of Ref. [30], it follows that

$$\begin{aligned}S(\rho)&=S\left(\sum_{k_1=0}^{s_1-1}\sum_{k_2=0}^{s_2-1}\dots\sum_{k_n=0}^{s_n-1}\nu_{1,k_1}\nu_{2,k_2}\dots\nu_{n,k_n}\right.\\&\quad\left.\times\left[\frac{1}{n}(\rho_{1,k_1}+\cdots+\rho_{n,k_n})\right]\right)\\&\geqslant\sum_{k_1=0}^{s_1-1}\sum_{k_2=0}^{s_2-1}\dots\sum_{k_n=0}^{s_n-1}\nu_{1,k_1}\nu_{2,k_2}\dots\nu_{n,k_n}S\left(\frac{\rho_{1,k_1}+\cdots+\rho_{n,k_n}}{n}\right)\\&\geqslant\min_{\substack{0\leqslant k_1\leqslant s_1-1\\ \vdots\\ 0\leqslant k_n\leqslant s_n-1}}S\left(\frac{\rho_{1,k_1}+\cdots+\rho_{n,k_n}}{n}\right)\\&=S\left(\frac{\rho_{1,t_1}+\cdots+\rho_{n,t_n}}{n}\right),\end{aligned} \tag{A65}$$

where $t_1\in\{0,\dots,s_1-1\},\dots,t_n\in\{0,\dots,s_n-1\}$.

On the other hand, while $\rho_1=\rho_{1,t_1}$, …, $\rho_n=\rho_{n,t_n}$, the equation of the linear dimension witness $\sum_{x=1}^{n}\mathrm{tr}(\rho_x M^{(x)})=w_d$ holds according to Eq. (A62).

Then considering that $\{\rho_{x,t_x}\}$ are rank-1 density matrices, they can be written as

$$\rho_{x,t_x}=|\Psi_x\rangle\langle\Psi_x|\quad\text{while } 1\leqslant x\leqslant n. \tag{A66}$$

Let

$$|\Psi_1'\rangle = |\Psi_1\rangle, \tag{A67}$$

$$|\Psi_2'\rangle = \frac{|\Psi_2\rangle - \langle\Psi_1'|\Psi_2\rangle|\Psi_1'\rangle}{\||\Psi_2\rangle - \langle\Psi_1'|\Psi_2\rangle|\Psi_1'\rangle\|}, \tag{A68}$$

$$|\Psi_3'\rangle = \frac{|\Psi_3\rangle - \langle\Psi_1'|\Psi_3\rangle|\Psi_1'\rangle - \langle\Psi_2'|\Psi_3\rangle|\Psi_2'\rangle}{\||\Psi_3\rangle - \langle\Psi_1'|\Psi_3\rangle|\Psi_1'\rangle - \langle\Psi_2'|\Psi_3\rangle|\Psi_2'\rangle\|}, \quad \ldots = \ldots, \tag{A69}$$

$$|\Psi_n'\rangle = \frac{|\Psi_n\rangle - \langle\Psi_1'|\Psi_n\rangle|\Psi_1'\rangle - \langle\Psi_2'|\Psi_n\rangle|\Psi_2'\rangle - \cdots - \langle\Psi_{n-1}'|\Psi_n\rangle|\Psi_{n-1}'\rangle}{\||\Psi_n\rangle - \langle\Psi_1'|\Psi_n\rangle|\Psi_1'\rangle - \langle\Psi_2'|\Psi_n\rangle|\Psi_2'\rangle - \cdots - \langle\Psi_{n-1}'|\Psi_n\rangle|\Psi_{n-1}'\rangle\|}. \tag{A70}$$

Then $\{|\Psi_1'\rangle, \ldots, |\Psi_n'\rangle\}$ are orthogonal pairwise and $\{|\Psi_1\rangle, \ldots, |\Psi_n\rangle\}$ are in the space $\Sigma = \mathrm{span}\{|\Psi_1'\rangle, \ldots, |\Psi_n'\rangle\}$. Since Eq. (A66), $\rho_{1,t_1}, \rho_{2,t_2}, \ldots, \rho_{n,t_n}$ are all in the space Σ. Since $\dim(\Sigma) \leqslant n$, Σ is included in $\mathbb{C}^n$.

Hence, given the value of a linear dimension witness, $\sum_{x=1}^n \mathrm{tr}(\rho_x M^{(x)}) = w_d$, for any density matrices $\{\rho_1, \ldots, \rho_n\}$, there exist density matrices $\{\rho_{1,t_1}, \ldots, \rho_{1,t_n}\}$, subject to

$$\mathrm{rank}(\rho_{x,t_x}) = 1 \quad \text{while } 1 \leqslant x \leqslant n, \tag{A71}$$

$$\rho_{x,t_x} \in \mathbb{C}^n \quad \text{while } 1 \leqslant x \leqslant n, \tag{A72}$$

$$\sum_{x=1}^{n} \mathrm{tr}\left(\rho_{x,t_x} M^{(x)}\right) = w_d, \tag{A73}$$

$$S\left(\frac{\rho_{1,t_1} + \cdots + \rho_{n,t_n}}{n}\right) \leqslant S\left(\frac{\rho_1 + \cdots + \rho_n}{n}\right). \tag{A74}$$

Hence, given the value of a linear dimension witness, $\sum_{x=1}^n \sum_{y=1}^l \alpha_{xy}\, \mathrm{tr}(\rho_x M_y) = w_d$, the minimal value of the Von Neumann entropy $S(\rho)$, where $\rho = (\rho_1 + \cdots + \rho_n)/n$, is equal to

$$\min S\left(\frac{\rho_1 + \cdots + \rho_n}{n}\right) \quad \text{s.t.} \quad \sum_{x=1}^{n}\sum_{y=1}^{l} \alpha_{xy}\, \mathrm{tr}(\rho_x M_y) = w_d,$$
$$\mathrm{rank}\,(\rho_x) = 1 \quad \text{while } 1 \leqslant x \leqslant n, \quad \rho_x \in \mathbb{C}^n \quad \text{while } 1 \leqslant x \leqslant n. \tag{A75}$$

■

APPENDIX B: DETAILS ABOUT THE MAXIMAL DIFFERENCES BETWEEN MINIMAL VALUES OF $H(M)$ AND $S(\rho)$ FOR I_3, I_4, AND R_4

The states ρ_x, the measurements M_y, the deterministic expectation values $E_{m,y}^{(\lambda)}$, the deterministic probability distributions $P_{m,x}^{(\lambda)}$, and the efficiency matrix $A_{x,y}$ are written as

$$\rho_x = |\psi_x\rangle\langle\psi_x|, \tag{B1}$$

$$M_y = 1 - 2|m_y\rangle\langle m_y|, \tag{B2}$$

$$E_{m,y}^{(\lambda)} = \begin{bmatrix} E(m=0, y=1, \lambda) & \cdots & E(m=n-1, y=1, \lambda) \\ & \vdots & \\ E(m=0, y=l, \lambda) & \ldots & E(m=n-1, y=l, \lambda) \end{bmatrix}, \tag{B3}$$

$$P_{m,x}^{(\lambda)} = \begin{bmatrix} P(m=0|x=1, \lambda) & \cdots & P(m=0|x=n, \lambda) \\ & \vdots & \\ P(m=n-1|x=1, \lambda) & \cdots & P(m=n-1|x=n, \lambda) \end{bmatrix}, \tag{B4}$$

$$A_{xy} = \begin{bmatrix} \alpha_{x=1,y=1} & \cdots & \alpha_{x=1,y=l} \\ & \vdots & \\ \alpha_{x=n,y=1} & \cdots & \alpha_{x=n,y=l} \end{bmatrix}. \tag{B5}$$

Here we notice that $P_{m,x}^{(\lambda)}$ has n rows and $E_{m,y}^{(\lambda)}$ has n columns, since the message M with dimension n is proved to be sufficient in Sec. III of the Supplemental Material of Ref. [17]. While $\mathrm{rank}\{P_{m,x}^{(\lambda)}\}$ is less than n, the dimension witness of w_d can be obtained by a system with a dimension lower than n.

For the quantum entropy,

$$S(\rho) = -\operatorname{tr}(\rho \log_2 \rho), \quad \text{where } \rho = \sum_{x=1}^{n} \rho_x/n. \tag{B6}$$

For the classical entropy,

$$\begin{aligned} H(M) &= -\sum_{m=0}^{n-1} p_m \log_2 p_m, \quad \text{where } p_m \\ &= \sum_{x=1}^{n} \sum_{\lambda} P(m|x,\lambda) q_\lambda / n. \end{aligned} \tag{B7}$$

For the quantum dimension witness,

$$w_d^{(q)} = \sum_{x=1}^{n} \sum_{y=1}^{l} \alpha_{xy} \operatorname{tr}(\rho_x M_y). \tag{B8}$$

For the classical dimension witness,

$$\begin{aligned} w_d^{(c)} &= \sum_{x=1}^{n} \sum_{y=1}^{l} \alpha_{xy} \sum_{m=0}^{n-1} \sum_{\lambda} E(y,m,\lambda) P(m|x,\lambda) q_\lambda \\ &= \sum_{\lambda} \operatorname{tr}\left\{A_{xy} E_{m,y}^{(\lambda)} P_{m,x}^{(\lambda)}\right\} q_\lambda. \end{aligned} \tag{B9}$$

While accessing the values shown in Table I of the main text, the details about the states $|\psi_x\rangle$, the projection states $|m_y\rangle$, the deterministic expectation values $E_{m,y}^{(\lambda)}$, the deterministic probability distributions $P_{m,x}^{(\lambda)}$, and the probability of strategies q_λ are shown below.

1. For the case of I_3

The efficiency matrix is

$$A_{xy} = \begin{bmatrix} 1 & 1 \\ 1 & -1 \\ -1 & 0 \end{bmatrix}. \tag{B10}$$

The quantum states are

$$|\psi_1\rangle = (1,0,0), \tag{B11}$$

$$|\psi_2\rangle = (0.7972,0.6037,0), \tag{B12}$$

$$|\psi_3\rangle = (0.6511,-0.7590,0). \tag{B13}$$

The projection states are

$$|m_1\rangle = (0.4531,-0.8914,0), \tag{B14}$$

$$|m_2\rangle = (0.4451,0.8955,0). \tag{B15}$$

There are two classical strategies, λ_1 and λ_2, and their probabilities are

$$q_{\lambda_1} = 0.3111, \tag{B16}$$

$$q_{\lambda_2} = 0.6889. \tag{B17}$$

The deterministic expectation values are

$$E_{m,y}^{(\lambda_1)} = E_{m,y}^{(\lambda_2)} = \begin{bmatrix} 1 & 1 & -1 \\ 1 & -1 & 1 \end{bmatrix}. \tag{B18}$$

The deterministic probability distributions are

$$P_{m,x}^{(\lambda_1)} = \begin{bmatrix} 1 & 0 & 0 \\ 0 & 1 & 0 \\ 0 & 0 & 1 \end{bmatrix}, \tag{B19}$$

$$P_{m,x}^{(\lambda_2)} = \begin{bmatrix} 1 & 0 & 1 \\ 0 & 1 & 0 \\ 0 & 0 & 0 \end{bmatrix}. \tag{B20}$$

Substitute Eqs. (B10)–(B20) into Eqs. (B6)–(B9), we have

$$\begin{aligned} w_d^{(c)} = w_d^{(q)} &= 3.622, \\ H(M) &= 1.334 \text{ bit}, \\ S(\rho) &= 0.897 \text{ bit}. \end{aligned} \tag{B21}$$

2. For the case of I_4

The efficiency matrix is

$$A_{xy} = \begin{bmatrix} 1 & 1 & 1 \\ 1 & 1 & -1 \\ 1 & -1 & 0 \\ -1 & 0 & 0 \end{bmatrix}. \tag{B22}$$

The quantum states are

$$|\psi_1\rangle = (1,0,0,0), \tag{B23}$$

$$|\psi_2\rangle = (0.8323,0.5543,0,0), \tag{B24}$$

$$|\psi_3\rangle = (0.3108,0.9505,0,0), \tag{B25}$$

$$|\psi_4\rangle = (0.7623,0.5247,0.2148,0.3121). \tag{B26}$$

The projection states are

$$|m_1\rangle = (0.1692,0.1164,0.5549,0.8062), \tag{B27}$$

$$|m_2\rangle = (0.0750,-0.9972,0,0), \tag{B28}$$

$$|m_3\rangle = (0.4721,0.8816,0,0). \tag{B29}$$

There are two classical strategies, λ_1 and λ_2, and their probabilities are

$$q_{\lambda_1} = 0.3802, \tag{B30}$$

$$q_{\lambda_2} = 0.6198. \tag{B31}$$

The deterministic expectation values are

$$E_{m,y}^{(\lambda_1)} = E_{m,y}^{(\lambda_2)} = \begin{bmatrix} 1 & 1 & 1 & -1 \\ 1 & 1 & -1 & 1 \\ 1 & -1 & 1 & 1 \end{bmatrix}. \tag{B32}$$

The deterministic probability distributions are

$$P_{m,x}^{(\lambda_1)} = \begin{bmatrix} 1 & 0 & 0 & 1 \\ 0 & 1 & 0 & 0 \\ 0 & 0 & 1 & 0 \\ 0 & 0 & 0 & 0 \end{bmatrix}, \tag{B33}$$

$$P_{m,x}^{(\lambda_2)} = \begin{bmatrix} 1 & 0 & 1 & 1 \\ 0 & 1 & 0 & 0 \\ 0 & 0 & 0 & 0 \\ 0 & 0 & 0 & 0 \end{bmatrix}. \tag{B34}$$

Substitute Eqs. (B22)–(B34) into Eqs. (B6)–(B9), we have

$$\begin{aligned} w_d^{(c)} = w_d^{(q)} &= 5.760, \\ H(M) &= 1.223 \text{ bit}, \\ S(\rho) &= 0.829 \text{ bit}. \end{aligned} \tag{B35}$$

3. For the case of R_4

The efficiency matrix is

$$A_{xy} = \begin{bmatrix} 1 & 1 \\ 1 & -1 \\ -1 & 1 \\ -1 & -1 \end{bmatrix}. \tag{B36}$$

The quantum states are

$$|\psi_1\rangle = (1,0,0,0), \tag{B37}$$

$$|\psi_2\rangle = (0.7588, 0.2363 - 0.6070i, 0, 0), \tag{B38}$$

$$|\psi_3\rangle = (0.7588, 0.2363 + 0.6070i, 0, 0), \tag{B39}$$

$$|\psi_4\rangle = (0.3893, 0.9211, 0, 0). \tag{B40}$$

The projection states are

$$|m_1\rangle = (0.1515 - 0.3891i, 0.9087, 0, 0), \tag{B41}$$

$$|m_2\rangle = (0.1515 + 0.3891i, 0.9087, 0, 0). \tag{B42}$$

There are two classical strategies, λ_1 and λ_2, and their probabilities are

$$q_{\lambda_1} = 0.6056, \tag{B43}$$

$$q_{\lambda_2} = 0.3944. \tag{B44}$$

The deterministic expectation values are

$$E_{m,y}^{(\lambda_1)} = E_{m,y}^{(\lambda_2)} = \begin{bmatrix} 1 & 1 & -1 & -1 \\ 1 & -1 & 1 & -1 \end{bmatrix}. \tag{B45}$$

The deterministic probability distributions are

$$P_{m,x}^{(\lambda_1)} = \begin{bmatrix} 1 & 0 & 1 & 0 \\ 0 & 1 & 0 & 0 \\ 0 & 0 & 0 & 0 \\ 0 & 0 & 0 & 1 \end{bmatrix}, \tag{B46}$$

$$P_{m,x}^{(\lambda_2)} = \begin{bmatrix} 1 & 1 & 1 & 0 \\ 0 & 0 & 0 & 0 \\ 0 & 0 & 0 & 0 \\ 0 & 0 & 0 & 1 \end{bmatrix}. \tag{B47}$$

Substitute Eqs. (B36)–(B47) into Eqs. (B6)–(B9)

$$\begin{aligned} w_d^{(c)} = w_d^{(q)} &= 5.211 \\ H(M) &= 1.356 \text{ bit} \\ S(\rho) &= 0.888 \text{ bit} \end{aligned} \tag{B48}$$

APPENDIX C: THE ROTATION ANGLES OF HWPS AND QWPS

1. The preparation of quantum states

Following Eq. (7) in the main text and Eqs. (B11)–(B13), we get Table II.

Following Eq. (7) in the main text and Eqs. (B23)–(B26), we get Table III.

Following Eq. (7) in the main text and Eqs. (B37)–(B40), we get Table IV.

TABLE II. The rotation angles of HWPs and QWP in the state preparator for quantum states in the case of I_3.

	$h_s^{(p)}$	$q_s^{(p)}$	$h_i^{(p)}$
$\|\psi_1\rangle$	0°	0°	0°
$\|\psi_2\rangle$	18.57°	37.14°	0°
$\|\psi_3\rangle$	−24.69°	−49.38°	0°

TABLE III. The rotation angles of HWPs and QWP in the state preparator for quantum states in the case of I_4.

	$h_s^{(p)}$	$q_s^{(p)}$	$h_i^{(p)}$
$\|\psi_1\rangle$	0°	0°	0°
$\|\psi_2\rangle$	16.83°	33.66°	0°
$\|\psi_3\rangle$	35.95°	71.89°	0°
$\|\psi_4\rangle$	17.27°	34.54°	11.13°

TABLE IV. The rotation angles of HWPs and QWP in the state preparator for quantum states in the case of R_4.

	$h_s^{(p)}$	$q_s^{(p)}$	$h_i^{(p)}$
$\|\psi_1\rangle$	0°	0°	0°
$\|\psi_2\rangle$	33.55°	33.55°	0°
$\|\psi_3\rangle$	0°	33.55°	0°
$\|\psi_4\rangle$	33.55°	67.09°	0°

TABLE V. The rotation angles of HWPs and QWP in the state preparator for classical states of strategy λ_1 in the case of I_3.

	$h_s^{(p)}$	$q_s^{(p)}$	$h_i^{(p)}$
State 1	0°	0°	0°
State 2	45°	90°	0°
State 3	45°	90°	45°

TABLE VI. The rotation angles of HWPs and QWP in the state preparator for classical states of strategy λ_2 in the case of I_3.

	$h_s^{(p)}$	$q_s^{(p)}$	$h_i^{(p)}$
State 1	0°	0°	0°
State 2	45°	90°	0°
State 3	0°	0°	0°

TABLE VII. The rotation angles of HWPs and QWP in the state preparator for classical states of strategy λ_1 in the case of I_4.

	$h_s^{(p)}$	$q_s^{(p)}$	$h_i^{(p)}$
State 1	0°	0°	0°
State 2	45°	90°	0°
State 3	45°	90°	45°
State 4	0°	0°	0°

TABLE VIII. The rotation angles of HWPs and QWP in the state preparator for classical states of strategy λ_2 in the case of I_4.

	$h_s^{(p)}$	$q_s^{(p)}$	$h_i^{(p)}$
State 1	0°	0°	0°
State 2	45°	90°	0°
State 3	0°	0°	0°
State 4	0°	0°	0°

TABLE IX. The rotation angles of HWPs and QWP in the state preparator for classical states of strategy λ_1 in the case of R_4.

	$h_s^{(p)}$	$q_s^{(p)}$	$h_i^{(p)}$
State 1	0°	0°	0°
State 2	45°	90°	0°
State 3	0°	0°	0°
State 4	0°	0°	45°

TABLE X. The rotation angles of HWPs and QWP in the state preparator for classical states of strategy λ_2 in the case of R_4.

	$h_s^{(p)}$	$q_s^{(p)}$	$h_i^{(p)}$
State 1	0°	0°	0°
State 2	0°	0°	0°
State 3	0°	0°	0°
State 4	0°	0°	45°

TABLE XI. The rotation angles of HWPs and QWPs in the measurement device for detection of quantum states in the case of I_3.

	$h_s^{(m)}$	$q_s^{(m)}$	$h_i^{(m)}$	$q_i^{(m)}$
$\lvert m_1\rangle$	−31.53°	−63.06°	0°	0°
$\lvert m_2\rangle$	31.79°	63.57°	0°	0°

TABLE XII. The rotation angles of HWPs and QWPs in the measurement device for detection of quantum states in the case of I_4.

	$h_s^{(p)}$	$q_s^{(p)}$	$h_i^{(p)}$	$q_i^{(m)}$
$\lvert m_1\rangle$	17.26°	34.53°	39.07°	78.15°
$\lvert m_2\rangle$	−42.85°	−85.70°	0°	0°
$\lvert m_3\rangle$	30.92°	61.84°	0°	0°

2. The preparation of classical states

Following Eq. (7) in the main text and Eqs. (B19)–(B20), we get Tables V and VI.

Following Eq. (7) in the main text and Eqs. (B33)–(B34), we get Tables VII and VIII.

Following Eq. (7) in the main text and Eqs. (B46)–(B47), we get Tables IX and X.

3. The detection of quantum dimension witness

The expectations of detect-events for the quantum dimension witness in the case of I_3, I_4, and R_4 are

$$E = \frac{-D_{a,b} + D_{c,b} + D_{c,d}}{D_{a,b} + D_{c,b} + D_{c,d}} \quad \text{for } I_3, \tag{C1}$$

$$E = \frac{-D_{a,b} + D_{c,b} + D_{c,d} + D_{a,d}}{D_{a,b} + D_{c,b} + D_{c,d} + D_{a,d}} \quad \text{for } I_4, \tag{C2}$$

$$E = \frac{-D_{a,b} + D_{c,b} + D_{c,d} + D_{a,d}}{D_{a,b} + D_{c,b} + D_{c,d} + D_{a,d}} \quad \text{for } R_4. \tag{C3}$$

Following Eq. (8) in the main text and Eqs. (B14)–(B15), we get Table XI.

Following Eq. (8) in the main text and Eqs. (B27)–(B29), we get Table XII.

Following Eq. (8) in the main text and Eqs. (B41)–(B42), we get Table XIII.

4. The detection of classical dimension witness

Following Eq. (B18), the expectations of detection events for the classical dimension witness in the case of I_3 are

$$E = \frac{D_{a,b} + D_{c,b} - D_{c,d}}{D_{a,b} + D_{c,b} + D_{c,d}} \quad \text{for } M_1, \tag{C4}$$

$$E = \frac{D_{a,b} - D_{c,b} + D_{c,d}}{D_{a,b} + D_{c,b} + D_{c,d}} \quad \text{for } M_2. \tag{C5}$$

Following Eq. (B32), the expectations of detection events for the classical dimension witness in the case of I_4

TABLE XIII. The rotation angles of HWPs and QWPs in the measurement device for detection of quantum states in the case of R_4.

	$h_s^{(p)}$	$q_s^{(p)}$	$h_i^{(p)}$	$q_i^{(m)}$
$\lvert m_1\rangle$	50.52°	78.54°	0°	0°
$\lvert m_2\rangle$	28.02°	78.54°	0°	0°

TABLE XIV. The rotation angles of HWPs and QWPs in the measurement device in the case of I_3.

	$h_s^{(m)}$	$q_s^{(m)}$	$h_i^{(m)}$	$q_i^{(m)}$
$D_{a,b}(\|\nu_1\rangle)$	0°	0°	0°	0°
$D_{a,b}(\|\nu_2\rangle)$	45°	0°	0°	0°
$D_{a,b}(\|\nu_3\rangle)$	45°	0°	45°	0°
$D_{a,b}(\|\nu_4\rangle)$	45°	0°	22.5°	0°
$D_{a,b}(\|\nu_5\rangle)$	45°	0°	22.5°	45°
$D_{a,b}(\|\nu_6\rangle)$	22.5°	45°	22.5°	45°
$D_{a,b}(\|\nu_7\rangle)$	22.5°	45°	22.5°	90°
$D_{a,b}(\|\nu_8\rangle)$	22.5°	45°	0°	90°
$D_{a,b}(\|\nu_9\rangle)$	22.5°	0°	0°	90°

are

$$E=\frac{D_{a,b}+D_{c,b}+D_{c,d}-D_{a,d}}{D_{a,b}+D_{c,b}+D_{c,d}+D_{a,d}}\quad \text{for } M_1, \tag{C6}$$

$$E=\frac{D_{a,b}+D_{c,b}-D_{c,d}+D_{a,d}}{D_{a,b}+D_{c,b}+D_{c,d}+D_{a,d}}\quad \text{for } M_2, \tag{C7}$$

$$E=\frac{D_{a,b}-D_{c,b}+D_{c,d}+D_{a,d}}{D_{a,b}+D_{c,b}+D_{c,d}+D_{a,d}}\quad \text{for } M_3. \tag{C8}$$

Following Eq. (B45), the expectations of detection events for the classical dimension witness in the case of R_4 are

$$E=\frac{D_{a,b}+D_{c,b}-D_{c,d}-D_{a,d}}{D_{a,b}+D_{c,b}+D_{c,d}+D_{a,d}}\quad \text{for } M_1, \tag{C9}$$

$$E=\frac{D_{a,b}-D_{c,b}+D_{c,d}-D_{a,d}}{D_{a,b}+D_{c,b}+D_{c,d}+D_{a,d}}\quad \text{for } M_2. \tag{C10}$$

The rotation angles of HWPs and QWPs in the measurement device for classical states in the cases of I_3, I_4, and R_4 are all 0°.

TABLE XV. The rotation angles of HWPs and QWPs in the measurement device in the cases of I_4 and R_4.

	$h_s^{(m)}$	$q_s^{(m)}$	$h_i^{(m)}$	$q_i^{(m)}$
$D_{a,b}(\|\nu_1\rangle)$	45°	0°	45°	0°
$D_{a,b}(\|\nu_2\rangle)$	45°	0°	0°	0°
$D_{a,b}(\|\nu_3\rangle)$	0°	0°	0°	0°
$D_{a,b}(\|\nu_4\rangle)$	0°	0°	45°	0°
$D_{a,b}(\|\nu_5\rangle)$	22.5°	0°	45°	0°
$D_{a,b}(\|\nu_6\rangle)$	22.5°	0°	0°	0°
$D_{a,b}(\|\nu_7\rangle)$	22.5°	45°	0°	0°
$D_{a,b}(\|\nu_8\rangle)$	22.5°	45°	45°	0°
$D_{a,b}(\|\nu_9\rangle)$	22.5°	45°	22.5°	0°
$D_{a,b}(\|\nu_{10}\rangle)$	22.5°	45°	22.5°	45°
$D_{a,b}(\|\nu_{11}\rangle)$	22.5°	0°	22.5°	45°
$D_{a,b}(\|\nu_{12}\rangle)$	45°	0°	22.5°	45°
$D_{a,b}(\|\nu_{13}\rangle)$	0°	0°	22.5°	45°
$D_{a,b}(\|\nu_{14}\rangle)$	0°	0°	22.5°	90°
$D_{a,b}(\|\nu_{15}\rangle)$	45°	0°	22.5°	90°
$D_{a,b}(\|\nu_{16}\rangle)$	22.5°	0°	22.5°	90°

5. The detection of quantum entropy

In quantum state tomography, for the reconstruction of an s order density matrix, s^2 projection states $|\nu_j\rangle$ are utilized where their projective operators are linearly independent. These projection states are realized by rotating angles of $h_s^{(m)}$, $q_s^{(m)}$, $h_i^{(m)}$, and $q_i^{(m)}$ following Eq. (8) in the main text. We get Table XIV for I_3 and Table XV for I_4 and R_4. The detection event $D_{a,b}(|\nu_j\rangle)$, which represents the coincidence number between ports a and b while the projection state is $|\nu_j\rangle$, is

$$D_{a,b}(|\nu_j\rangle)=N\langle\nu_j|\rho_x|\nu_j\rangle\quad \text{while } 1\leqslant j\leqslant s^2. \tag{C11}$$

N is a constant. Since ρ has s^2-1 independent variables, it can be linearly reconstructed by $D_{a,b}(|\nu_j\rangle)$:

$$\rho_x=\frac{\sum_{j=1}^{s^2}M_jD_{a,b}(|\nu_j\rangle)}{\sum_{j=1}^{s}D_{a,b}(|\nu_j\rangle)}. \tag{C12}$$

$M_j(1\leqslant j\leqslant s^2)$ are the matrices which depend on $|\nu_j\rangle$. To keep the positive semidefiniteness of ρ_x, the maximum likelihood estimation [24] is used.

For the case of I_3, $s=3$ and each of ρ_1, ρ_2, and ρ_3 is a 3×3 density matrix. We reconstruct ρ_1, ρ_2, and ρ_3 and then obtain the average state as

$$\rho=\tfrac{1}{3}(\rho_1+\rho_2+\rho_3). \tag{C13}$$

The matrices M_j $(1\leqslant j\leqslant 9)$ are as follows:

$$M_1=\frac{1}{2}\begin{bmatrix}2&-1+i&0\\-1-i&0&0\\0&0&0\end{bmatrix},$$

$$M_2=\frac{1}{2}\begin{bmatrix}0&-1+i&1-i\\-1-i&2&-1+i\\1+i&-1-i&0\end{bmatrix},$$

$$M_3=\frac{1}{2}\begin{bmatrix}0&0&-2i\\0&0&-1+i\\2i&-1-i&2\end{bmatrix},\quad M_4=\begin{bmatrix}0&0&i\\0&0&-i\\-i&i&0\end{bmatrix},$$

$$M_5=\begin{bmatrix}0&0&-1\\0&0&1\\-1&1&0\end{bmatrix},\quad M_6=\begin{bmatrix}0&0&2\\0&0&0\\2&0&0\end{bmatrix},$$

$$M_7=\begin{bmatrix}0&0&2i\\0&0&0\\-2i&0&0\end{bmatrix},\quad M_8=\begin{bmatrix}0&1&-1-i\\1&0&0\\-1+i&0&0\end{bmatrix},$$

$$M_9=\begin{bmatrix}0&-i&0\\i&0&0\\0&0&0\end{bmatrix}. \tag{C14}$$

For the case of I_4 and R_4, $s=4$ and each of ρ_1, ρ_2, ρ_3, and ρ_4 is a 4×4 density matrix. We reconstruct ρ_1, ρ_2, ρ_3, and ρ_4 and then obtain the average state as

$$\rho=\tfrac{1}{4}(\rho_1+\rho_2+\rho_3+\rho_4). \tag{C15}$$

The matrices M_j $(1\leqslant j\leqslant 16)$ are as follows:

$$M_1=\frac{1}{2}\begin{bmatrix}0&0&1&0\\0&0&-1-i&i\\1&-1+i&2&-1-i\\0&-i&-1+i&0\end{bmatrix},$$

$$M_2 = \frac{1}{2}\begin{bmatrix} 0 & -1+i & 1 & 0 \\ -1-i & 2 & -1-i & i \\ 1 & -1+i & 0 & 0 \\ 0 & -i & 0 & 0 \end{bmatrix},$$

$$M_3 = \frac{1}{2}\begin{bmatrix} 2 & -1+i & 1 & -1-i \\ -1-i & 0 & 0 & i \\ 1 & 0 & 0 & 0 \\ -1+i & -i & 0 & 0 \end{bmatrix},$$

$$M_4 = \frac{1}{2}\begin{bmatrix} 0 & 0 & 1 & -1-i \\ 0 & 0 & 0 & i \\ 1 & 0 & 0 & -1-i \\ -1+i & -i & -1+i & 2 \end{bmatrix},$$

$$M_5 = \frac{1}{2}\begin{bmatrix} 0 & 0 & -1+i & 0 \\ 0 & 0 & 0 & 1-i \\ -1-i & 0 & 0 & 2i \\ 0 & 1+i & -2i & 0 \end{bmatrix},$$

$$M_6 = \frac{1}{2}\begin{bmatrix} 0 & -2i & -1+i & 0 \\ 2i & 0 & 0 & 1-i \\ -1-i & 0 & 0 & 0 \\ 0 & 1+i & 0 & 0 \end{bmatrix},$$

$$M_7 = \frac{1}{2}\begin{bmatrix} 0 & 2 & -1+i & 0 \\ 2 & 0 & 0 & -1+i \\ -1-i & 0 & 0 & 0 \\ 0 & -1-i & 0 & 0 \end{bmatrix},$$

$$M_8 = \frac{1}{2}\begin{bmatrix} 0 & 0 & -1+i & 0 \\ 0 & 0 & 0 & -1+i \\ -1-i & 0 & 0 & 2 \\ 0 & -1-i & 2 & 0 \end{bmatrix},$$

$$M_9 = \begin{bmatrix} 0 & 0 & -i & 0 \\ 0 & 0 & 0 & -i \\ i & 0 & 0 & 0 \\ 0 & i & 0 & 0 \end{bmatrix},$$

$$M_{10} = \begin{bmatrix} 0 & 0 & 1 & 0 \\ 0 & 0 & 0 & 1 \\ 1 & 0 & 0 & 0 \\ 0 & 1 & 0 & 0 \end{bmatrix},$$

$$M_{11} = \begin{bmatrix} 0 & 0 & -i & 0 \\ 0 & 0 & 0 & i \\ i & 0 & 0 & 0 \\ 0 & -i & 0 & 0 \end{bmatrix},$$

$$M_{12} = \frac{1}{2}\begin{bmatrix} 0 & 0 & -1+i & 0 \\ 0 & 0 & 2 & -1-i \\ -1-i & 2 & 0 & 0 \\ 0 & -1+i & 0 & 0 \end{bmatrix},$$

$$M_{13} = \frac{1}{2}\begin{bmatrix} 0 & 0 & -1+i & 2 \\ 0 & 0 & 0 & -1-i \\ -1-i & 0 & 0 & 0 \\ 2 & -1+i & 0 & 0 \end{bmatrix},$$

$$M_{14} = \frac{1}{2}\begin{bmatrix} 0 & 0 & -1-i & 2i \\ 0 & 0 & 0 & 1-i \\ -1+i & 0 & 0 & 0 \\ -2i & 1+i & 0 & 0 \end{bmatrix},$$

$$M_{15} = \frac{1}{2}\begin{bmatrix} 0 & 0 & -1-i & 0 \\ 0 & 0 & 2i & 1-i \\ -1+i & -2i & 0 & 0 \\ 0 & 1+i & 0 & 0 \end{bmatrix},$$

$$M_{16} = \begin{bmatrix} 0 & 0 & 1 & 0 \\ 0 & 0 & 0 & -1 \\ 1 & 0 & 0 & 0 \\ 0 & -1 & 0 & 0 \end{bmatrix}. \tag{C16}$$

6. The detection of classical entropy

We only need to record the distribution of the click number of each detection event while all rotation angles of HWPs and QWPs are 0°.

APPENDIX D: COUNTEREXAMPLES FOR THE HYPOTHESES IN DISCUSSION OF THE MAIN TEXT

Hypothesis 1. $\min_{\rho_x\in\mathbb{C}^d} S(\rho) = \min_{\rho_x\in\mathbb{C}^n} S(\rho)$ while $\sum_{x=1}^n \sum_{y=1}^l \alpha_{xy}\,\mathrm{tr}(\rho_x M_y) = w_d$, $\rho = \sum_{x=1}^n \rho_x/n$, and $L_{d-1}^{(q)} < w_d \leqslant L_d^{(q)}$ $(d<n)$, where $L_d^{(q)}$ is the d-dimensional quantum bound of the dimension witness w_d.

Counterexample 1. From Eq. (3) of the main text, the dimension witness I_4 can be written as

$$\begin{aligned} I_4 &= \mathrm{tr}[\rho_1(M_1+M_2+M_3)] + \mathrm{tr}[\rho_2(M_1+M_2-M_3)] \\ &\quad + \mathrm{tr}[\rho_3(M_1-M_2)] + \mathrm{tr}[\rho_1(-M_1)] \\ &\leqslant \lambda_{\max}(M_1+M_2+M_3) + \lambda_{\max}(M_1+M_2-M_3) \\ &\quad + \lambda_{\max}(M_1-M_2) + \lambda_{\max}(-M_1), \end{aligned} \tag{D1}$$

where $\lambda_{\max}(\Omega)$ represents the maximum eigenvalue of observable Ω.

Let $M_k = 2\hat{U}^{-1}|m_k\rangle\langle m_k|\hat{U} - 1$, where $\hat{U}$ is a second-order unitary matrix and $1 \leqslant k \leqslant 3$. Since $\{|m_k\rangle\}$ are in $\mathbb{C}^2$, without loss of generality, let

$$|m_1\rangle = (1,0), \tag{D2}$$

$$|m_2\rangle = \left(\cos\frac{\theta}{2}, \sin\frac{\theta}{2}\right) \quad \text{while } \theta \in [0,\pi], \tag{D3}$$

$$|m_3\rangle = \left(\cos\frac{\phi}{2}, \sin\frac{\phi}{2}e^{i\varphi}\right), \quad \text{while} \quad \phi \in (-\pi,\pi] \quad \text{and} \quad \varphi \in [0,\pi). \tag{D4}$$

Then

$$M_1+M_2+M_3 = \hat{U}^{-1}\begin{bmatrix} 1+\cos\theta+\cos\phi & \sin\theta+\sin\phi e^{i\varphi} \\ \sin\theta+\sin\phi e^{-i\varphi} & -1-\cos\theta-\cos\phi \end{bmatrix}\hat{U}, \tag{D5}$$

$$M_1+M_2-M_3 = \hat{U}^{-1}\begin{bmatrix} 1+\cos\theta-\cos\phi & \sin\theta-\sin\phi e^{i\varphi} \\ \sin\theta-\sin\phi e^{-i\varphi} & -1-\cos\theta+\cos\phi \end{bmatrix}\hat{U}, \tag{D6}$$

$$M_1-M_2 = \hat{U}^{-1}\begin{bmatrix} 1-\cos\theta & -\sin\theta \\ -\sin\theta & -1+\cos\theta \end{bmatrix}\hat{U}, \tag{D7}$$

$$-M_1 = \hat{U}^{-1}\begin{bmatrix} -1 & 0 \\ 0 & 1 \end{bmatrix}\hat{U}. \tag{D8}$$

Hence,

$$\lambda_{\max}(M_1+M_2+M_3)=\sqrt{(3+2\cos\theta)+(2\cos\theta\cos\phi+2\sin\theta\sin\phi\cos\varphi)}, \tag{D9}$$

$$\lambda_{\max}(M_1+M_2-M_3)=\sqrt{(3+2\cos\theta)-(2\cos\theta\cos\phi+2\sin\theta\sin\phi\cos\varphi)}, \tag{D10}$$

$$\lambda_{\max}(M_1-M_2)=\sqrt{2-2\cos\theta}, \tag{D11}$$

$$\lambda_{\max}(-M_1)=1. \tag{D12}$$

Substituting Eqs. (D9)–(D12) into Eq. (D1), we get

$$\begin{aligned}I_4 &\leqslant \sqrt{(3+2\cos\theta)+(2\cos\theta\cos\phi+2\sin\theta\sin\phi\cos\varphi)}\\ &\quad+\sqrt{(3+2\cos\theta)-(2\cos\theta\cos\phi+2\sin\theta\sin\phi\cos\varphi)}+\sqrt{2-2\cos\theta}+1\\ &\leqslant 2\sqrt{(3+2\cos\theta)}+\sqrt{2-2\cos\theta}+1\\ &=\frac{1}{2}\sqrt{(3+2\cos\theta)}+\frac{1}{2}\sqrt{(3+2\cos\theta)}+\frac{1}{2}\sqrt{(3+2\cos\theta)}+\frac{1}{2}\sqrt{(3+2\cos\theta)}+\sqrt{2-2\cos\theta}+1\\ &\leqslant\sqrt{5\left[\frac{3+2\cos\theta}{4}+\frac{3+2\cos\theta}{4}+\frac{3+2\cos\theta}{4}+\frac{3+2\cos\theta}{4}+(2-2\cos\theta)\right]}+1=6.\end{aligned} \tag{D13}$$

The second sign of less than or equal to ($\leqslant$) becomes equal to ($=$) if

$$2\cos\theta\cos\phi+2\sin\theta\sin\phi\cos\varphi=0. \tag{D14}$$

The third sign of less than or equal to ($\leqslant$) becomes equal to ($=$) if

$$\tfrac{1}{2}\sqrt{(3+2\cos\theta)}=\sqrt{2-2\cos\theta}\Rightarrow\cos\theta=0.5. \tag{D15}$$

Considering Eq. (D3), from Eq. (D15) we can obtain

$$\theta=\frac{\pi}{3}. \tag{D16}$$

On the other hand, the vectors $\{|v_k\rangle\}$, where $\rho_k=\hat{U}^{-1}|v_k\rangle\langle v_k|\hat{U}$, should be the eigenvectors corresponding to the maximum eigenvalues of Eqs.(D5)–(D8). Hence,

$$|v_1\rangle=\frac{(1+\cos\theta+\cos\phi+\sqrt{(1+\cos\theta+\cos\phi)^2+|\sin\theta+\sin\phi e^{i\varphi}|^2},\sin\theta+\sin\phi e^{-i\varphi})}{\sqrt{2[(1+\cos\theta+\cos\phi)^2+|\sin\theta+\sin\phi e^{i\varphi}|^2]+2(1+\cos\theta+\cos\phi)\sqrt{(1+\cos\theta+\cos\phi)^2+|\sin\theta+\sin\phi e^{i\varphi}|^2}}}, \tag{D17}$$

$$|v_2\rangle=\frac{(1+\cos\theta-\cos\phi+\sqrt{(1+\cos\theta-\cos\phi)^2+|\sin\theta-\sin\phi e^{i\varphi}|^2},\sin\theta-\sin\phi e^{-i\varphi})}{\sqrt{2[(1+\cos\theta-\cos\phi)^2+|\sin\theta-\sin\phi e^{i\varphi}|^2]+2(1+\cos\theta-\cos\phi)\sqrt{(1+\cos\theta-\cos\phi)^2+|\sin\theta-\sin\phi e^{i\varphi}|^2}}}, \tag{D18}$$

$$|v_3\rangle=\frac{(1-\cos\theta+\sqrt{(1-\cos\theta)^2+|\sin\theta|^2},-\sin\theta)}{\sqrt{2[(1-\cos\theta)^2+|\sin\theta|^2]+2(1-\cos\theta)\sqrt{(1-\cos\theta)^2+|\sin\theta|^2}}}, \tag{D19}$$

$$|v_3\rangle=(0,1). \tag{D20}$$

Substituting Eqs. (D14) and (D16) into Eqs. (D17)–(D20), we get

$$\rho_1=\hat{U}^{-1}|v_1\rangle\langle v_1|\hat{U}=\hat{U}^{-1}\frac{1}{8}\begin{bmatrix}7+2\cos\phi & \sqrt{3}+2\sin\phi e^{-i\varphi}\\ \sqrt{3}+2\sin\phi e^{i\varphi} & 1-2\cos\phi\end{bmatrix}\hat{U}, \tag{D21}$$

$$\rho_2=\hat{U}^{-1}|v_2\rangle\langle v_2|\hat{U}=\hat{U}^{-1}\frac{1}{8}\begin{bmatrix}7-2\cos\phi & \sqrt{3}-2\sin\phi e^{-i\varphi}\\ \sqrt{3}-2\sin\phi e^{i\varphi} & 1+2\cos\phi\end{bmatrix}\hat{U}, \tag{D22}$$

$$\rho_3=\hat{U}^{-1}|v_3\rangle\langle v_3|\hat{U}=\hat{U}^{-1}\frac{1}{4}\begin{bmatrix}3 & -\sqrt{3}\\ -\sqrt{3} & 1\end{bmatrix}\hat{U}, \tag{D23}$$

$$\rho_4=\hat{U}^{-1}|v_4\rangle\langle v_4|\hat{U}=\hat{U}^{-1}\begin{bmatrix}0 & 0\\ 0 & 1\end{bmatrix}\hat{U}. \tag{D24}$$

Hence,

$$\rho = \frac{1}{4}(\rho_1 + \rho_2 + \rho_3 + \rho_4) = \hat{U}^{-1}\frac{1}{8}\begin{bmatrix}5 & 0\\ 0 & 3\end{bmatrix}\hat{U}. \quad \text{(D25)}$$

For $I_4 = L_2^{(q)} = 6$, although ϕ, φ, and $\hat{U}$ are not unique, the Von Neumann entropy of ρ is unique. Then while $I_4 = 6$,

$$\min_{\rho_x \in \mathbb{C}^2} S(\rho) = 0.954 \text{ bit}. \quad \text{(D26)}$$

On the other hand, there exist states for ququarts,

$$|\psi_1\rangle = (1,0,0,0), \quad \text{(D27)}$$

$$|\psi_2\rangle = (0.8290,0.5592,0,0), \quad \text{(D28)}$$

$$|\psi_3\rangle = (0.7660,-0.6428,0,0), \quad \text{(D29)}$$

$$|\psi_4\rangle = (0.8844,-0.0191,-0.1204,0.4506), \quad \text{(D30)}$$

and the measurement operators $M_y = 1 - 2|m_y\rangle\langle m_y|$,

$$|m_1\rangle = (0.2229,-0.0058,-0.2516,0.9418), \quad \text{(D31)}$$

$$|m_2\rangle = (0.4838,-0.8752,0,0), \quad \text{(D32)}$$

$$|m_3\rangle = (0.4695,0.8829,0,0), \quad \text{(D33)}$$

where $I_4 = 6.000$ and $S(\rho) = 0.912$ bit. Hence,

$$\min_{\rho_x \in \mathbb{C}^4} S(\rho) \leqslant 0.9122 \text{ bit}. \quad \text{(D34)}$$

From Eqs. (D26) and (D34), we get

$$\min_{\rho_x \in \mathbb{C}^2} S(\rho) > \min_{\rho_x \in \mathbb{C}^4} S(\rho), \quad \text{(D35)}$$

which disproves the hypothesis.

Counterexample 2. For $R_4 = L_3^{(q)} = 6.472$, there are sets of states ρ_x in $\mathbb{C}^3$ [14]. The states are $\rho_x = \hat{U}^{-1}|\psi_x\rangle\langle\psi_x|\hat{U}$, where $\hat{U}$ is a third-order unitary matrix and

$$|\psi_1\rangle = (0,0,1), \quad \text{(D36)}$$

$$|\psi_2\rangle = \left(\frac{1}{\sqrt{2}},-\frac{1}{\sqrt{2}},0\right), \quad \text{(D37)}$$

$$|\psi_3\rangle = \left(\frac{1}{\sqrt{2}},\frac{1}{\sqrt{2}},0\right), \quad \text{(D38)}$$

$$|\psi_4\rangle = (1,0,0). \quad \text{(D39)}$$

The measurement operators are $M_y = 1 - 2\hat{U}^{-1}|m_y\rangle\langle m_y|\hat{U}$, where

$$|m_1\rangle = \left(\frac{\sqrt{5}+1}{\sqrt{10+2\sqrt{5}}},\frac{2}{\sqrt{10+2\sqrt{5}}},0\right), \quad \text{(D40)}$$

$$|m_2\rangle = \left(\frac{\sqrt{5}+1}{\sqrt{10+2\sqrt{5}}},\frac{-2}{\sqrt{10+2\sqrt{5}}},0\right). \quad \text{(D41)}$$

Although $\hat{U}$ is not unique, the Von Neumann entropy of ρ is unique. Then while $R_4 = 6.472$,

$$\min_{\rho_x \in \mathbb{C}^3} S(\rho) = 1.5 \text{ bit}. \quad \text{(D42)}$$

On the other hand, there exist states for ququarts,

$$|\psi_1\rangle = (1,0,0,0), \quad \text{(D43)}$$

$$|\psi_2\rangle = (0.5892,0.5736,0.5690,0), \quad \text{(D44)}$$

$$|\psi_3\rangle = (-0.6257,0.5584,0.0293,0.5439), \quad \text{(D45)}$$

$$|\psi_4\rangle = (0.0175,0.9998,0,0), \quad \text{(D46)}$$

and the measurement operators $M_y = 1 - 2|m_y^{(1)}\rangle\langle m_y^{(1)}| - 2|m_y^{(2)}\rangle\langle m_y^{(2)}|$,

$$\left|m_1^{(1)}\right\rangle = (-0.2925,0.8860,-0.0987,0.3460), \quad \text{(D47)}$$

$$\left|m_1^{(2)}\right\rangle = (-0.1432,-0.3525,0.3117,0.8707), \quad \text{(D48)}$$

$$\left|m_2^{(1)}\right\rangle = (0.2906,0.8847,0.3496,-0.1030), \quad \text{(D49)}$$

$$\left|m_2^{(2)}\right\rangle = (0.1143,-0.3604,0.8911,0.2511), \quad \text{(D50)}$$

where $R_4 = 6.472$ and $S(\rho) = 1.418$ bit. Hence,

$$\min_{\rho_x \in \mathbb{C}^4} S(\rho) \leqslant 1.418 \text{ bit}. \quad \text{(D51)}$$

From Eqs. (D42) and (D51), we get

$$\min_{\rho_x \in \mathbb{C}^3} S(\rho) > \min_{\rho_x \in \mathbb{C}^4} S(\rho), \quad \text{(D52)}$$

which also disproves the hypothesis. This is also shown in Fig. 3 in the Supplemental Material of Ref. [17].

Hypothesis 2. For any linear dimension witness $\sum_{x=1}^{n}\sum_{y=1}^{l}\alpha_{xy}\,\mathrm{tr}(\rho_x M_y) = w_d$, the right-hand side of Eq. (11) in Ref. [17] is the minimal classical entropy.

Let $\lambda_{i,j}$ be the jth strategy for an i-dimensional classical system. $w(\lambda_{i,j})$ represents the classical dimension witness,

$$w(\lambda_{i,j}) = \sum_{x=1}^{n}\sum_{y=1}^{l}\alpha_{xy}E_{xy}^{(\lambda_{i,j})}. \quad \text{(D53)}$$

The maximal value of the dimension witness for the d-dimensional classical system is L_d, hence

$$L_d = \max_j w(\lambda_{d,j}). \quad \text{(D54)}$$

Here, we use $H([p_0,p_1,\ldots,p_{n-2},p_{n-1}])$ to represent the classical entropy $H(M)$. Without loss of generality, let $p_0 \geqslant p_1 \geqslant \cdots \geqslant p_{n-2} \geqslant p_{n-1}$. Then

$$H([p_0,p_1,\ldots,p_{n-2},p_{n-1}]) = H(M) = \sum_{k=0}^{n-1} -p_k\log_2 p_k. \quad \text{(D55)}$$

For the case of the d-dimensional system where $d < n$, $p_k = 0$ while $d \leqslant k \leqslant n-1$. Then we use $\lim_{x\to 0} x\log_2 x = 0$ to keep the effectivity of Eq. (D55).

Counterexample 3. Let

$$A_{xy}=\begin{bmatrix}\alpha_{x=1,y=1} & \alpha_{x=1,y=2}\\ \alpha_{x=2,y=1} & \alpha_{x=2,y=2}\\ \alpha_{x=3,y=1} & \alpha_{x=3,y=2}\\ \alpha_{x=4,y=1} & \alpha_{x=4,y=2}\end{bmatrix}=\begin{bmatrix}0.4955 & 0.7775\\ -0.6092 & -0.6572\\ 0.0048 & -0.5283\\ -0.5877 & 0.8258\end{bmatrix}. \tag{D56}$$

Then the maximal value of the dimension witness by the four-dimensional classical system is $L_4 = 4.4860$, while

$$E^{(\lambda_{4,1})}_{m,y}=\begin{bmatrix}E(m=0,y=1,\lambda_{4,1}) & \dots & E(m=3,y=1,\lambda_{4,1})\\ E(m=0,y=2,\lambda_{4,1}) & \dots & E(m=3,y=2,\lambda_{4,1})\end{bmatrix}=\begin{bmatrix}1 & -1 & 1 & -1\\ 1 & -1 & -1 & 1\end{bmatrix} \tag{D57}$$

and

$$P^{(\lambda_{4,1})}_{m,x}=\begin{bmatrix}P(m=0|x=1,\lambda_{4,1}) & \dots & P(m=0|x=4,\lambda_{4,1})\\ & \vdots & \\ P(m=3|x=1,\lambda_{4,1}) & \dots & P(m=3|x=4,\lambda_{4,1})\end{bmatrix}=\begin{bmatrix}1&0&0&0\\0&1&0&0\\0&0&1&0\\0&0&0&1\end{bmatrix}. \tag{D58}$$

The maximal value of the dimension witness by the three-dimensional classical system is $L_3 = 4.4764$, while

$$E^{(\lambda_{3,1})}_{m,y}=\begin{bmatrix}E(m=0,y=1,\lambda_{3,1}) & \dots & E(m=3,y=1,\lambda_{3,1})\\ E(m=0,y=2,\lambda_{3,1}) & \dots & E(m=3,y=2,\lambda_{3,1})\end{bmatrix}=\begin{bmatrix}-1 & 1 & -1 & 1\\ -1 & 1 & 1 & -1\end{bmatrix} \tag{D59}$$

and

$$P^{(\lambda_{3,1})}_{m,x}=\begin{bmatrix}P(m=0|x=1,\lambda_{3,1}) & \dots & P(m=0|x=4,\lambda_{3,1})\\ & \vdots & \\ P(m=3|x=1,\lambda_{3,1}) & \dots & P(m=3|x=4,\lambda_{3,1})\end{bmatrix}=\begin{bmatrix}0&1&1&0\\1&0&0&0\\0&0&0&1\\0&0&0&0\end{bmatrix}. \tag{D60}$$

The maximal value of the dimension witness by the two-dimensional classical system is $L_2^{(c)} = 3.4854$, while

$$E^{(\lambda_{2,1})}_{m,y}=\begin{bmatrix}E(m=0,y=1,\lambda_{2,1}) & \dots & E(m=3,y=1,\lambda_{2,1})\\ E(m=0,y=2,\lambda_{2,1}) & \dots & E(m=3,y=2,\lambda_{2,1})\end{bmatrix}=\begin{bmatrix}1 & -1 & 1 & -1\\ 1 & -1 & -1 & 1\end{bmatrix} \tag{D61}$$

and

$$P^{(\lambda_{2,1})}_{m,x}=\begin{bmatrix}P(m=0|x=1,\lambda_{2,1}) & \dots & P(m=0|x=4,\lambda_{2,1})\\ & \vdots & \\ P(m=3|x=1,\lambda_{2,1}) & \dots & P(m=3|x=4,\lambda_{2,1})\end{bmatrix}=\begin{bmatrix}1&0&0&1\\0&1&1&0\\0&0&0&0\\0&0&0&0\end{bmatrix}. \tag{D62}$$

The maximal value of the dimension witness by the one-dimensional classical system is $L_1 = 1.1144$, while

$$E^{(\lambda_{1,1})}_{m,y}=\begin{bmatrix}E(m=0,y=1,\lambda_{1,1}) & \dots & E(m=3,y=1,\lambda_{1,1})\\ E(m=0,y=2,\lambda_{1,1}) & \dots & E(m=3,y=2,\lambda_{1,1})\end{bmatrix}=\begin{bmatrix}-1 & -1 & 1 & 1\\ 1 & -1 & -1 & 1\end{bmatrix} \tag{D63}$$

and

$$P^{(\lambda_{1,1})}_{m,x}=\begin{bmatrix}P(m=0|x=1,\lambda_{1,1}) & \dots & P(m=0|x=4,\lambda_{1,1})\\ & \vdots & \\ P(m=3|x=1,\lambda_{1,1}) & \dots & P(m=3|x=4,\lambda_{1,1})\end{bmatrix}=\begin{bmatrix}1&1&1&1\\0&0&0&0\\0&0&0&0\\0&0&0&0\end{bmatrix}. \tag{D64}$$

For dimension witness $w_d = L_2$, the minimal classical entropy is $H([p_0,\dots,p_3])$, subject to

$$\sum_{x=1}^{4}\sum_{i=1}^{4}\sum_{j} q_{\lambda_{i,j}} P(m=k|x,\lambda_{i,j})/4 = p_k \quad \text{while } 0 \leqslant k \leqslant 3, \tag{D65}$$

$$\sum_{i=1}^{4}\sum_{j} q_{\lambda_{i,j}} w(\lambda_{i,j}) = L_2, \tag{D66}$$

$$\sum_{i=1}^{4}\sum_{j} q_{\lambda_{i,j}} = 1. \tag{D67}$$

Following Eqs. (D66), (D67), and (D54),

$$\begin{aligned}L_2 &\leqslant \sum_{i=1}^{4}\sum_j q_{\lambda_{i,j}} \max_j w(\lambda_{i,j}) = \sum_{i=1}^{4}\sum_j q_{\lambda_{i,j}} L_i = \sum_j q_{\lambda_{1,j}} L_1\\ &+ \left(1-\sum_j q_{\lambda_{1,j}} - \sum_j q_{\lambda_{3,j}} - \sum_j q_{\lambda_{4,j}}\right) L_2 + \sum_j q_{\lambda_{3,j}} L_3 + \sum_j q_{\lambda_{4,j}} L_4\\ &\Rightarrow \sum_j q_{\lambda_{1,j}} \leqslant \frac{L_3-L_2}{L_2-L_1}\sum_j q_{\lambda_{3,j}} + \frac{L_4-L_2}{L_2-L_1}\sum_j q_{\lambda_{4,j}} = 0.4180\sum_j q_{\lambda_{3,j}} + 0.4220\sum_j q_{\lambda_{4,j}}. \end{aligned} \tag{D68}$$

Then, for p_0,

$$p_0 = \sum_{x=1}^{4}\sum_\lambda q_\lambda P(m=0|x,\lambda)/4 = \sum_{i=1}^{4}\sum_j q_{\lambda_{i,j}}\left\{\sum_{x=1}^{4} P(m=0|x,\lambda_{i,j})/4\right\}. \tag{D69}$$

Considering that, for different dimensional systems, $\sum_{x=1}^{4} P(m=0|x,\lambda_{i,j})/4$ have different upper bounds, $\sum_{x=1}^{4} P(m=0|x,\lambda_{1,j})/4 \leqslant 1$ for one-dimensional systems, $\sum_{x=0}^{4} P(m=0|x,\lambda_{2,j})/4 \leqslant 3/4$ for two-dimensional systems, $\sum_{x=1}^{4} P(m=0|x,\lambda_{3,j})/4 \leqslant 1/2$ for three-dimensional systems, and $\sum_{x=1}^{4} P(m=0|x,\lambda_{4,j})/4 \leqslant 1/4$ for four-dimensional systems. Here we notice that $\sum_{x=1}^{4} P(m=0|x,\lambda_{2,1})/4 \leqslant 1/2$ for the case of $\lambda_{2,1}$ from Eq. (D62). Hence

$$\begin{aligned}p_0 &\leqslant \sum_j q_{\lambda_{1,j}} 1 + \sum_{j\neq 2} q_{\lambda_{2,j}}\frac{3}{4} + q_{\lambda_{2,1}}\frac{1}{2} + \sum_j q_{\lambda_{3,j}}\frac{1}{2} + \sum_j q_{\lambda_{4,j}}\frac{1}{4} = \frac{3}{4} - \frac{1}{4}q_{\lambda_{2,1}} + \frac{1}{4}\left[\sum_j q_{\lambda_{1,j}} - \sum_j q_{\lambda_{3,j}} - 2\sum_j q_{\lambda_{4,j}}\right]\\ &= \frac{3}{4} - \frac{1}{4}q_{\lambda_{2,1}} + \frac{1}{4}\left[\sum_j q_{\lambda_{1,j}} - 0.4180\sum_j q_{\lambda_{3,j}} - 0.4220\sum_j q_{\lambda_{4,j}}\right] - \frac{0.5820}{4}\sum_j q_{\lambda_{3,j}} - \frac{1.5780}{4}\sum_j q_{\lambda_{4,j}}\\ &\leqslant \frac{3}{4} - \frac{1}{4}q_{\lambda_{2,1}} - \frac{0.5820}{4}\sum_j q_{\lambda_{3,j}} - \frac{1.5780}{4}\sum_j q_{\lambda_{4,j}}. \end{aligned} \tag{D70}$$

Because of Eq. (D66), $q_{\lambda_{2,1}}$, $\sum_j q_{\lambda_{3,j}}$, and $\sum_j q_{\lambda_{4,j}}$ can't be 0 simultaneously, therefore

$$p_0 < \tfrac{3}{4}. \tag{D71}$$

Since $p_0 \geqslant p_1 \geqslant p_2 \geqslant p_3$ and $w_d = L_2 > L_1$,

$$p_0 > \tfrac{1}{4}. \tag{D72}$$

Since $-x\log_2 x - y\log_2 y \geqslant -(x+y)\log_2(x+y)$ while $x \geqslant 0$, $y \geqslant 0$, and $x+y \leqslant 1$, then

$$H([p_0,p_1,p_2,p_3]) \geqslant H([p_0,p_1+p_2+p_3,0,0]). \tag{D73}$$

Since $-x\log_2 x - (1-x)\log_2(1-x) > -y\log_2 y - (1-y)\log_2(1-y)$ while $x \geqslant 0$, $y \geqslant 0$, and $0 < x < y \leqslant \frac{1}{2}$, then considering Eqs. (D71) and (D72),

$$H([p_0,p_1+p_2+p_3,0,0]) > H\left(\left[\tfrac{3}{4},\tfrac{1}{4},0,0\right]\right) = -\tfrac{3}{4}\log_2\tfrac{3}{4} - \tfrac{1}{4}\log_2\tfrac{1}{4} = 0.811 \text{ bit}. \tag{D74}$$

Hence

$$H([p_0,p_1,p_2,p_3]) > 0.811 \text{ bit}. \tag{D75}$$

On the other hand, while using the strategy of Eq. (11) in Ref. [17], for the case of $w_d = L_2^{(c)} = 3.4854$, the minimal classical entropy $H(M)$ is 0.811 bit. Hence, the hypothesis is disproved.

[1] A. Acín, N. Brunner, N. Gisin, S. Massar, S. Pironio, and V. Scarani, Phys. Rev. Lett. **98**, 230501 (2007).
[2] A. K. Ekert, Phys. Rev. Lett. **67**, 661 (1991).
[3] J.-D. Bancal, N. Gisin, Y.-C. Liang, and S. Pironio, Phys. Rev. Lett. **106**, 250404 (2011).
[4] R. Rabelo, M. Ho, D. Cavalcanti, N. Brunner, and V. Scarani, Phys. Rev. Lett. **107**, 050502 (2011).
[5] T. Moroder, J.-D. Bancal, Y.-C. Liang, M. Hofmann, and O. Gühne, Phys. Rev. Lett. **111**, 030501 (2013).
[6] J. T. Barreiro, J.-D. Bancal, P. Schindler, D. Nigg, M. Hennrich, T. Monz, N. Gisin, and R. Blatt, Nat. Phys. **9**, 559 (2013).
[7] N. Brunner, S. Pironio, A. Acin, N. Gisin, A. A. Méthot, and V. Scarani, Phys. Rev. Lett. **100**, 210503 (2008).
[8] R. Gallego, N. Brunner, C. Hadley, and A. Acín, Phys. Rev. Lett. **105**, 230501 (2010).
[9] J. Bowles, M. T. Quintino, and N. Brunner, Phys. Rev. Lett. **112**, 140407 (2014).
[10] M. Pawłowski and N. Brunner, Phys. Rev. A **84**, 010302 (2011).
[11] M. Hendrych, R. Gallego, M. Mičuda, N. Brunner, A. Acín, and J. P. Torres, Nat. Phys. **8**, 588 (2012).
[12] J. Ahrens, P. Badziąg, A. Cabello, and M. Bourennane, Nat. Phys. **8**, 592 (2012).
[13] V. D'Ambrosio, F. Bisesto, F. Sciarrino, J. F. Barra, G. Lima, and A. Cabello, Phys. Rev. Lett. **112**, 140503 (2014).
[14] J. Ahrens, P. Badziąg, M. Pawłowski, M. Żukowski, and M. Bourennane, Phys. Rev. Lett. **112**, 140401 (2014).
[15] A. Holevo, Prob. Peredachi Info. **9**, 3 (1973).
[16] M. Pawłowski, T. Paterek, D. Kaszlikowski, V. Scarani, A. Winter, and M. Żukowski, Nature (London) **461**, 1101 (2009).
[17] R. Chaves, J. B. Brask, and N. Brunner, Phys. Rev. Lett. **115**, 110501 (2015).
[18] J. Pearl, *Causality* (Cambridge University Press, Cambridge, England, 2009).
[19] R. Chaves, C. Majenz, and D. Gross, Nat. Commun. **6**, 5766 (2015).
[20] R. Chaves, L. Luft, T. O. Maciel, D. Gross, D. Janzing, and B. Schölkopf, in *Proceedings of the 30th Conference on Uncertainty in Artificial Intelligence* (AUAI, Corvallis, OR, 2014), p. 112.
[21] R. Chaves and T. Fritz, Phys. Rev. A **85**, 032113 (2012); T. Fritz and R. Chaves, IEEE Trans. Inf. Theory **59**, 803 (2013); R. Chaves, L. Luft, and D. Gross, New J. Phys. **16**, 043001 (2014).
[22] N. Harrigan, T. Rudolph, and S. Aaronson, arXiv:0709.1149; E. F. Galvao, Phys. Rev. A **80**, 022106 (2009).
[23] Y. I. Bogdanov, M. V. Chekhova, S. P. Kulik, G. A. Maslennikov, A. A. Zhukov, C. H. Oh, and M. K. Tey, Phys. Rev. Lett. **93**, 230503 (2004).
[24] D. F. V. James, P. G. Kwiat, W. J. Munro, and A. G. White, Phys. Rev. A **64**, 052312 (2001).
[25] R. T. Thew, K. Nemoto, A. G. White, and W. J. Munro, Phys. Rev. A **66**, 012303 (2002).
[26] Yu. I. Bogdanov, M. V. Chekhova, L. A. Krivitsky, S. P. Kulik, A. N. Penin, A. A. Zhukov, L. C. Kwek, C. H. Oh, and M. K. Tey, Phys. Rev. A **70**, 042303 (2004).
[27] H. Takesue and K. Inoue, Phys. Rev. A **70**, 031802 (2004).
[28] X. Li, P. L. Voss, J. E. Sharping, and P. Kumar, Phys. Rev. Lett. **94**, 053601 (2005).
[29] Q. Zhou, W. Zhang, J. Cheng, Y. Huang, and J. Peng, Opt. Lett. **34**, 2706 (2009).
[30] A. Wehrl, Rev. Mod. Phys. **50**, 221 (1978).